

Prototype Design and Analysis of the Performance of Hull Reservoir Wave Energy Converter (HRWEC) Under Random Sea Conditions

ME 406: Mechanical Engineering Group Project I Report

Submitted by

W.D.A.M. Somathilake, E/14/332

E. Somathilake, E/14/333

P.H.T.D. Weeraratne, E/14/369

Group No 12

in

partial fulfillment of the requirements for the degree
Bachelor of the Science of Engineering



**Department of Mechanical Engineering
Faculty of Engineering, University of Peradeniya**

02/12/2019

Executive summary

Wave Energy is a widespread, reliable renewable energy source. The early study on Wave Energy dates back in the 70's, with a particular effort in the last and present decade to make Wave Energy Converters (WECs) more profitable and predictable. HRWEC (Hull Reservoir Wave Energy Converter) is a flap-based WEC. The research activities described in the present work aim to develop a flap type Hull Reservoir Wave Energy converter for the calm wave conditions as well extreme wave conditions. The theoretical model was developed using rigid body equations for the Hull Reservoir (mooring lines included) and simulated through MATLAB in order to obtain the orientation and the position of the hull reservoir and the flap. Ultimately, the curves for average power capture vs the sea wave frequency were obtained for several damping constants. Using the obtained curves, the average power capture between Hull Reservoir Wave Energy Converter and PeWEC device is compared and contrasted.

The development of the preliminary design of the real scale device was done in order to make the device a reality. For that, previous prototype models were used This is an essential step before the detailed design of each and every part of the device.

Disclaimer

We declare that this report does not incorporate, without acknowledgement, any material previously submitted for any other Degree or Diploma to the best of my knowledge and belief, it does not contain any material previously published or written by another person or myself except where due references are made. It has not been accepted for any other course and is not being concurrently submitted to any other person.

W.D.A.M. Somathilake
E. Somathilake
P.H.T.D. Weerathne
02/12/2019

Table of Contents

Excutive summary	i
Disclaimer	ii
Table of Contents	iv
List of Figures	vi
List of Tables	vii
Abbreviations	viii
1 Introduction	1
2 Mathematical Modeling and Simulation	3
2.1 Equations of motion of the HRWEC	3
2.2 Hydrodynamic forces	5
2.3 Mooring model	6
2.4 Simulation of the motion of the HREWC	8
3 Preliminary Design	9
3.1 Determining physical dimensions	10
3.2 Development of the mechanisms	11
3.2.1 Hydraulic pump	11
3.2.2 Gear mechanism	12
3.3 Special Features	14
3.3.1 Aerodynamic roof	14
3.3.2 Double chamber design	14
3.4 Safety precautions	15
3.5 Possible problems	18
3.6 Materials used	19
4 Obtaining equations of motion for the device using rigid body equations	20
5 Results	21
6 Conclusion	26
7 Future Work	28
Acknowledgments	29
Appendices	30
Appendix A Mathematical Simulation of the HRWEC	30
A.1 Euler's method	30
A.2 Matlab Code	30
Appendix B Sea wavelength calculation	37
Appendix C Derivation of the equations of motion	38

List of Figures

1	SEAREV and its approximate model	1
2	Pendulum Wave energy Converter (PeWEC)	1
3	Hull Reservoir Wave Energy Converter	1
4	Flap type hull resevoir layout	3
5	Simplfied sketch of the device used to obtain the equations of motion	4
6	Lazy-s mooring model	6
7	Simplified mooring model	7
8	Simulated result in MATLAB	8
9	Main components of the device(a)	9
10	Main components of the device(b)	9
11	Dimensions of the device	11
12	Hydraulic pump concept	12
13	Axial pump unit	12
14	Geared piston pump set	12
15	Gear orientation	13
16	Ratchet mechanism	13
17	Configuration for double flap design	14
18	Gear mechanism with the internal gear	14
19	Forces acting on the device	15
20	Double chamber design	15
21	Safety belts and lanyards	15
22	Safety fence that can be used around subunits.	16
23	Good lighting at an offshore working environment	16
24	Steel grating flooring	17
25	Traction tread flooring	17
26	An offshore emergency alarm/ unit	17
27	Specific pathways with safety fences.	18
28	Emergency lifeboats used at offshore buildings.	18
29	Surge velocity variation with wave time period	21
30	Surge variation with wave time period	21
31	Heave velocity variation with wave time period	21
32	Heave variation with wave time period	22
33	Pitch velocity variation with wave time period	22
34	Pitch variation with wave time period	22
35	Flap velocity variation with wave time period	22
36	Flap angle variation with wave time period	23
37	Variation of Flap Angle With Time for Different Time Periods	23
38	Surge velocity variation with wave time period	23
39	Surge variation with wave time period	24
40	Heave velocity variation with wave time period	24
41	Heave variation with wave time period	24
42	Pitch velocity variation with wave time period	24
43	Pitch variation with wave time period	25
44	Flap velocity variation with wave time period	25
45	Flap angle variation with wave time period	25
46	Power variation with wave time period	25
47	Surge, heave and pitch velocity variation of the hull with time period	26
48	Surge, heave and pitch velocity variation of the hull with time period	26

49	Model of the device	38
50	Frames of reference	39

List of Tables

1	Features of the prototype device	4
2	Values of real and model instances	10

Abbreviations

HRWEC	Hull Reservoir Wave Energy Converter
PeWEC	Pendulum Wave Energy Converter
PTO	Power Take Off
WEC	Wave Energy Converter

1 Introduction

Currently the world is heading in the direction of developing renewable energy sources to replace the other non-renewable resources that is currently used to generate most of our energy. Therefore naturally, sea wave energy harnessing devices have become of a greater interest. There have been many researches to develop such devices and our focus in this current project is one of them.

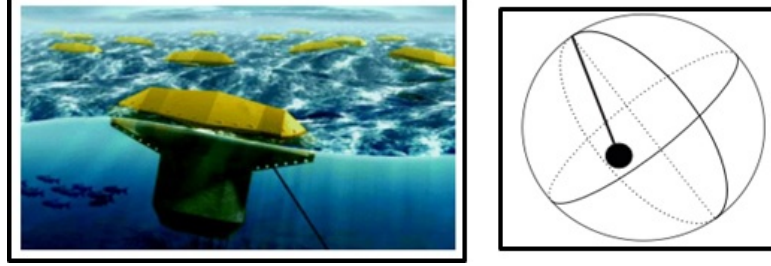


Figure 1: SEAREV and its approximate model

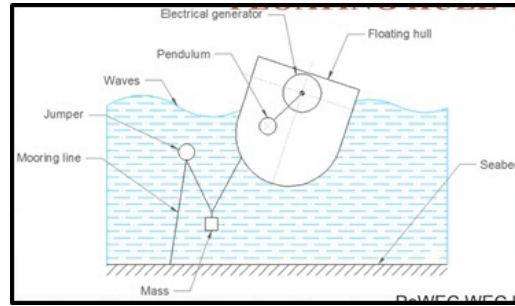


Figure 2: Pendulum Wave energy Converter (PeWEC)

Currently there are different types of devices to extract wave energy. Such as SEAREV which has an internal pendulum that has the ability to move in two degrees of freedom as shown in figure 1. Another device is the PeWEC as shown in figure 3 which has a pendulum that can rotate only about one axis relative to the hull and the behavior of this has been studied as it can be seen in [3] and [4].

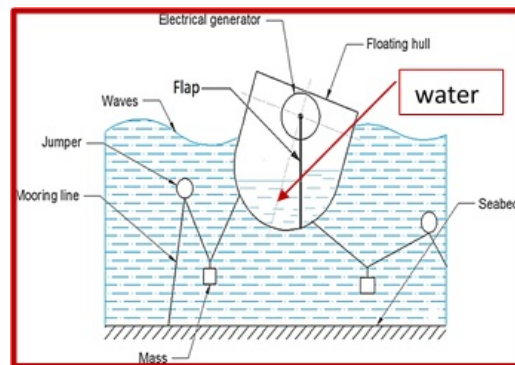


Figure 3: Hull Reservoir Wave Energy Converter

The device of interest is a hull reservoir with an internal flap as shown in the figure 3. It has water filled inside it up to a certain level unlike the PeWEC. The energy from the motion of the flap is used to produce electricity using a generator.

Developments in the modeling of the device has been done to the device up to a great extent as it can be seen in the [4] and [3]. Our objective in the project is to have model coupled with the ocean

waves. This has already been done but we have focused on developing a more general model with reduced amount of assumptions. That is the goal is to model and simulate a device for a more general case with higher degrees of freedom.

The motion of the model was simulated for the conditions given in [3] and [4] and the results obtained was compared with the existing results for validation and also, equations of motion for the device was derived in such a manner that with small modifications, the number of degrees of freedom can be easily increased. All these were carried out without any water inside the hull. The simulations were done using MATLAB.

The ultimate goal of this project is to develop a functioning WEC that can extract ocean energies in an effective manner. Therefore, the preliminary design of the actual device was also developed.

In the future, we expect to do a simulation after adding water inside the hull and also to carry out an experimental procedure to see how the model works in real life conditions and whether the experimental values match the theoretical ones.

2 Mathematical Modeling and Simulation

Initial step of the project was to simulate the HREWC in the conditions stated in [3] and [4] in similar conditions and compare the results obtained with the results in the papers. This helps us to verify whether the simulation done is accurate and if the coefficients used for the wave forces and added masses are corresponding to the ones used in [3] and [4]. The model of the device that is being mathematically simulated is as shown in figure 4.

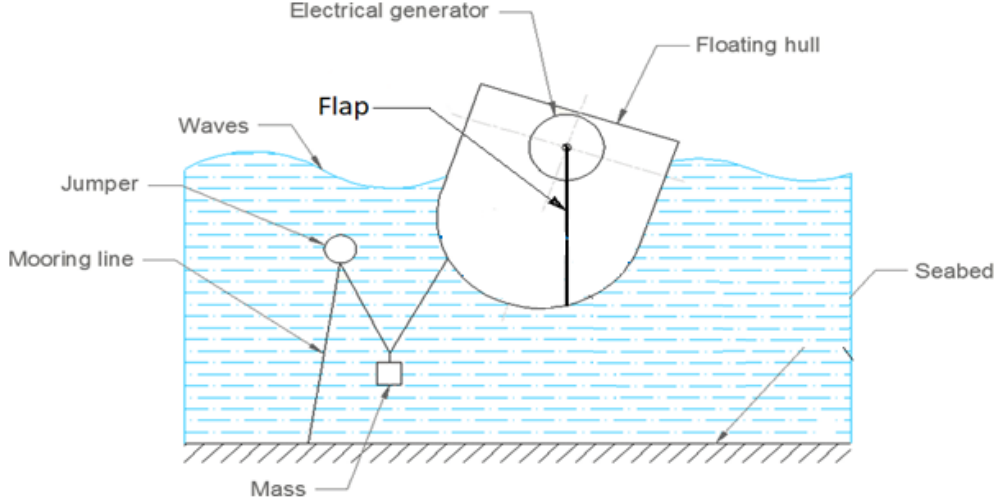


Figure 4: Flap type hull resevoir layout

For the calculations done in the [4], the device is considered to have a pendulum rather than a flap, but when there is no fluid inside the hull the flap behaves as a pendulum and therefore the same equations can be used to determine the dynamics of the flap type hull reservoir as well. Also, the HRWEC is connected to the ocean bed by a mooring system which must also be modeled to determine the forces acting from it on the hull.

2.1 Equations of motion of the HRWEC

The equations of motion of the device was obtained in [4] by using the Lagrange approach and the device was considered to have only 4 degrees of freedom. Which means it moves only in one plane(x-z plane), as shown in figure 5 therefore it can be seen that the surge, heave and pitch motions were considered but the sway roll and yaw motions were neglected. This is fairly accurate because the degrees of freedoms that has been neglected varies at transition motions and at steady state motion, their effect is minimal. As seen in the figure 5, θ is the pitch angle and α is the angle of rotation of the flap relative to the hull and the motion in x and z directions give the surge and heave motions respectively. Other parameters that are used and their respective values as given in [4] is shown in table 1

By using the Lagrange method the equations of motion for the prototype can be found in terms of the parameters in table 1. Therefore the equations of motion can be obtained here, M_{hp} takes into account the mass and inertial properties of flap and buoyant and M_c represents off diagonal terms relating the couplings between the flap and the hull then,

$$M_{hp} = \begin{bmatrix} m_f + m_b & 0 & 0 & 0 \\ 0 & m_f + m_b & 0 & 0 \\ 0 & 0 & I_b + I_f + m_f(d^2 + l^2) - 2m_f dl \cos \alpha & 0 \\ 0 & 0 & 0 & I_f + m_f l^2 \end{bmatrix}$$

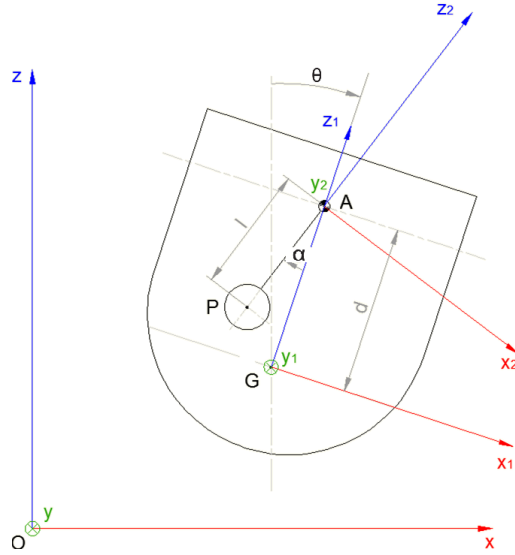


Figure 5: Simplified sketch of the device used to obtain the equations of motion

Symbol	Description	Value
Hull		
L	Length	$3m$
R	Radius	$1.5m$
W	Width	$2m$
m_b	Mass	$3176kg$
I_{xx}	Roll axis moment of inertia	$1499kgm^2$
$I_{yy} = I_b$	Pitch axis moment of inertia	$2168kgm^2$
I_{zz}	Yaw axis moment of inertia	$2761kgm^2$
d	Pendulum hinge- hull COG distance	$0.858m$
Pendulum		
m_p	Mass	$410kg$
I_y	Moment of inertia with respect to COG	$88.18kgm^2$
I	Length	$0.866m$
PTO		
T_{nom}	Rated Torque	$220Nm$
T_{max}	Maximum Torque	$800Mn$
V_n	Rated speed	$90rpm$
Mooring		
F_g	Net gravity force	$98N$
F_b	Net buoyancy force	$250N$
l_1	Line 1 length	$2m$
l_2	Line 2 length	$0.4m$
l_3	Line 3 length	$1.8m$

Table 1: Features of the prototype device

$$M_c = \begin{bmatrix} 0 & 0 & m_f[d \cos \theta - l \cos(\theta + \alpha)] & -m_f l \cos(\theta + \alpha) \\ 0 & 0 & -m_f[d \sin \theta - l \sin(\theta + \alpha)] & m_f l \sin(\theta + \alpha) \\ m_f[d \cos \theta - l \cos(\theta + \alpha)] & -m_f[d \sin \theta - l \sin(\theta + \alpha)] & 0 & I_f + m_f l^2 - m_f d l \cos \alpha \\ -m_f l \cos(\theta + \alpha) & m_f l \sin(\theta + \alpha) & I_f + m_f l^2 - m_f d l \cos \alpha & 0 \end{bmatrix}$$

Therefore the mass matrix of the system M_s ,

$$M_s = M_{hp} + M_c$$

If F_{cor} is the Coriolis action due to the motion of the flap hinge,

$$F_{cor} = \begin{bmatrix} m_f[l(\dot{\theta} + \dot{\alpha})^2 \sin(\theta + \alpha) - d\dot{\theta}^2 \sin \theta] \\ m_f[l(\dot{\theta} + \dot{\alpha})^2 \cos(\theta + \alpha) - d\dot{\theta}^2 \cos \theta] \\ -m_f dl \sin \theta [(\dot{\theta} + \dot{\alpha})^2 - \dot{\theta}^2] \\ -m_f dl \dot{\theta}^2 \sin \theta \end{bmatrix}$$

F_{gr} is the forces due to gravity, let $g = 9.81$ be the acceleration due to gravity

$$F_{gr} = \begin{bmatrix} 0 \\ 0 \\ -m_f g[d \sin \theta - l \sin(\alpha + \theta)] \\ m_f g l \sin(\theta + \alpha) \end{bmatrix}$$

D_{pto} is the damping matrix due to the power take off device, here c is the damping constant due to the motion of the flap relative to the hull.

$$D_{pto} = \begin{bmatrix} 0 & 0 & 0 & 0 \\ 0 & 0 & 0 & 0 \\ 0 & 0 & 0 & 0 \\ 0 & 0 & 0 & c \end{bmatrix}$$

Then the equation of motion of the device can be written as,

$$M_s \begin{bmatrix} \ddot{x} \\ \dot{z} \\ \ddot{\theta} \\ \ddot{\alpha} \end{bmatrix} + D_{pto} \begin{bmatrix} \dot{x} \\ \dot{z} \\ \dot{\theta} \\ \dot{\alpha} \end{bmatrix} + F_{gr} + F_{cor} = 0$$

This is the motion of the device when there is no external forces acting on the system therefore the hydrodynamic forces and the mooring forces must be determined to simulate the motion of the prototype model.

2.2 Hydrodynamic forces

As the model moves in water, a certain amount of water moves along with it and these act as added masses and damping to the system. these values varies with the wave frequency and the variation of each individual values of the added mass matrix and the damping matrix has been determined previously using analytical software and here, we used those values for the simulation directly. Similarly the hydrodynamic forces due to the waves, F_w are also obtained and they are taken to vary in a sinusoidal manner. If the added mass matrix is, M_{hydro} and the damping matrix is D_{hydro} , the new mass matrix can be taken as M and the new damping matrix can be taken as D . Then,

$$M = M_s + M_{hydro}$$

$$D = D_{pto} + D_{hydro}$$

Also during the simulation, when the device operates near resonant frequencies, the motion of the device becomes too large and therefore becomes unstable. To avoid this, an additional damping matrix D' was introduces which simulate other losses and hydrodynamic factors that has not been modeled

properly. But this can be taken to be reasonable as in real operating conditions, many losses can occur that is difficult to analytically evaluate. The primary objective is to find the resonant frequencies and since damping constants does not affect the natural frequencies of the body drastically, the resonant frequencies of the obtained results will not vary by much, but the amplitude will be affected and the constants were selected to match the data of [4] as much as possible. If D' is taken as,

$$D' = \begin{bmatrix} c_{\dot{x}} & 0 & 0 & 0 \\ 0 & c_{\dot{z}} & 0 & 0 \\ 0 & 0 & c_{\dot{\theta}} & 0 \\ 0 & 0 & 0 & 0 \end{bmatrix}$$

Here, $c_{\dot{x}}, c_{\dot{z}}$ and $c_{\dot{\theta}}$ are the damping constants for the surge, heave and pitch motions respectively. Hence the damping matrix must be modified as,

$$D = D_{pto} + D_{hydro} + D'$$

Also, restoring forces act on the device due to the hydrodynamic forces acting on the system, if these forces are given in matrix K ,

$$K = \begin{bmatrix} 0 \\ WL\rho gZ_s \\ \rho gV\theta\left(Z_B + \frac{I}{V}\right) \\ 0 \\ 0 \end{bmatrix}$$

Here,

$$I = \frac{4}{3} \frac{R}{2} \left(\frac{L}{2} \right)^2$$

and ρ is the density of water, V is the submerged volume, Z_s is the submerged volume, Z_B is the distance from the center of gravity to the center of buoyancy in z direction.

The other force that must be determined is the mooring forces acting on the hull.

2.3 Mooring model

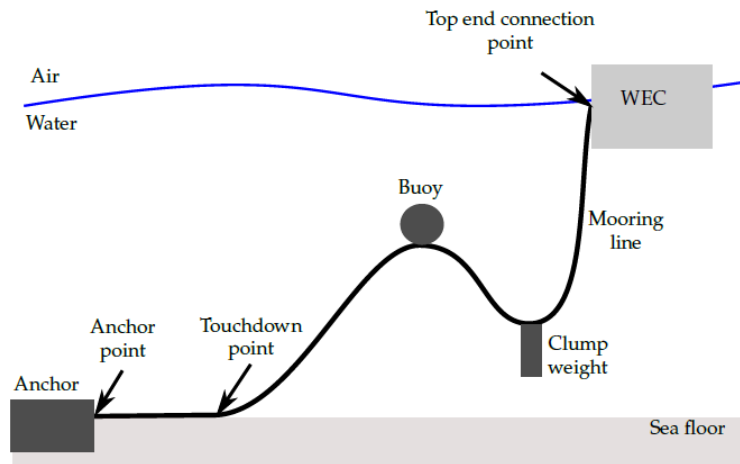


Figure 6: Lazy-s mooring model

As shown in [1], there are different types of mooring models that can be used and the one selected in [4] is the lazy-s models as shown in figure 6. In [1], the self weight of the cables and the variation

of the position of the cable is not taken as linear with the lower most cable lying along the sea bed up to the touchdown point.

But in [4], the net gravity force and the net buoyancy force is considered therefore, the resultant conditions of the buoy, clump weight, and the cables are taken, also the cables are taken to be straight lines connecting the anchor point to the buoy, the buoy to the weight and the weight to the WEC. Also the cables are taken to be of constant length. Therefore the mooring model considered here is as shown in figure 7 The equations for the static condition of the mooring system is obtained by

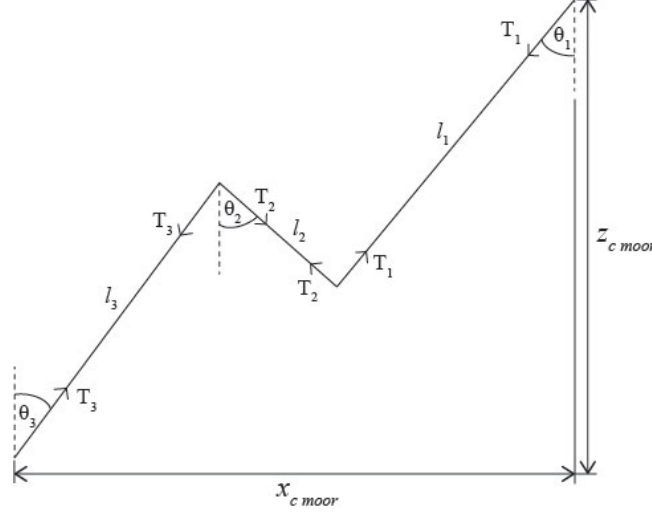


Figure 7: Simplified mooring model

considering the equilibrium at the buoy and the clump weight and by the distance from the point the mooring cable is fixed to the WEC and the anchor point.

$$\begin{aligned}
 T_1 \cos \theta_1 - T_2 \cos \theta_2 &= 0 \\
 T_1 \sin \theta_1 + T_2 \sin \theta_2 &= F_b \\
 T_2 \cos \theta_2 - T_3 \cos \theta_3 &= 0 \\
 T_2 \sin \theta_2 + T_3 \sin \theta_3 &= F_g \\
 l_1 \cos \theta_1 + l_2 \cos \theta_2 + l_3 \cos \theta_3 &= x_{c Moor} \\
 l_1 \sin \theta_1 - l_2 \sin \theta_2 + l_3 \sin \theta_3 &= z_{c Moor}
 \end{aligned}$$

Here, l_i and T_i are the length and the tension of the i^{th} rope ($i = 1, 2, 3$). Values for l_i ($i = 1, 2, 3$), F_b and F_g are given in table 1. Therefore, the tensions of the mooring cables and their respective orientations can be determined by solving the above equations numerically for the static equilibrium of the hull at a certain instance to determine the forces acting on it and the values obtained is used to calculate the motion of the hull until the mooring forces are determined again. If the horizontal and vertical forces acting on the hull is F_{mx} and F_{mz} respectively and the torque acting about y axis is T_{my} , The mooring force vector, F_{moor} is,

$$F_{moor} = \begin{bmatrix} -T_1 \sin(\theta_1) \\ -T_1 \cos(\theta_1) \\ T_{my} \\ 0 \end{bmatrix}$$

Where,

$$T_{my} = [0 \quad 1 \quad 0] \left(x_{moor} \times \begin{bmatrix} -T_1 \sin(\theta_1) \\ -T_1 \cos(\theta_1) \\ 0 \end{bmatrix} \right)$$

x_{moor} is vector from the center of mass of the hull to the point at which the mooring cable is connected to the hull.

2.4 Simulation of the motion of the HREWC

The simulation was done by solving the equations of motion of the HRWEC in matlab the equations were solved using the Euler's method as shown in A.1 and for this, the system of equations must be converted to a first order equations,

$$M \begin{bmatrix} \ddot{x} \\ \ddot{z} \\ \ddot{\theta} \\ \ddot{\alpha} \end{bmatrix} + D \begin{bmatrix} \dot{x} \\ \dot{z} \\ \dot{\theta} \\ \dot{\alpha} \end{bmatrix} + K + F_{gr} + F_{cor} = F_w + F_{moor}$$

$$\begin{bmatrix} M & 0_{4 \times 4} \\ 0_{4 \times 4} & I_{4 \times 4} \end{bmatrix} \begin{bmatrix} \ddot{x} \\ \ddot{z} \\ \ddot{\theta} \\ \ddot{\alpha} \end{bmatrix} + \begin{bmatrix} D & 0_{4 \times 4} \\ -I_{4 \times 4} & 0_{4 \times 4} \end{bmatrix} \begin{bmatrix} \dot{x} \\ \dot{z} \\ \dot{\theta} \\ \dot{\alpha} \end{bmatrix} = \begin{bmatrix} F_w + F_m - F_{gr} - F_{cor} \\ 0 \\ 0 \\ 0 \end{bmatrix}$$

$$A\dot{X} + BX = F$$

The MATLAB code in A.2 was used to solve and simulate the motion and obtain the necessary data to find the resonant frequencies and the average power output.

From [4], the average power output $P_{\alpha,avg}$ is given by

$$P_{\alpha,avg} = \frac{1}{2}(m_f l d) \omega^2 \theta_0 \alpha_0$$

Here ω is the wave frequency θ_0 and α_0 are the amplitudes of the hull pitch and the flap angle relative to the hull respectively.

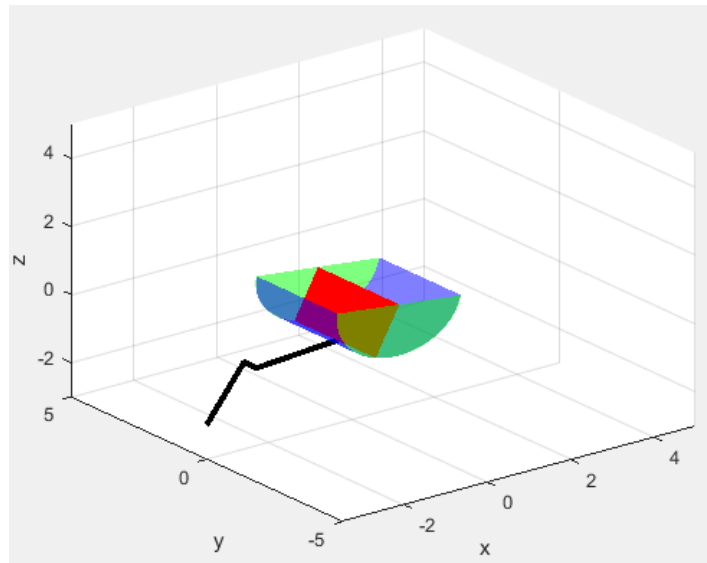


Figure 8: Simulated result in MATLAB

3 Preliminary Design

Preliminary design is the procedure before drafting the first detailed design. It is more of an Engineering design than a machine design therefore there is no one particular correct design and one cannot simply claim that they have achieved the optimum one.

In this section, the first step towards the commercial Hull Reservoir Wave Energy Converter is proposed. It includes the qualitative and quantitative idea of essential components, physical properties, useful mechanisms to convert wave energy and selection of materials.

The main components of the hull reservoir energy converter as shown in figures 9 and 10 are,

- Hull body
- Flaps
- Aerodynamic roof
- Reservoir pump
- Electricity generator
- Power plant floor
- Motion transmission system.
- Mooring lines

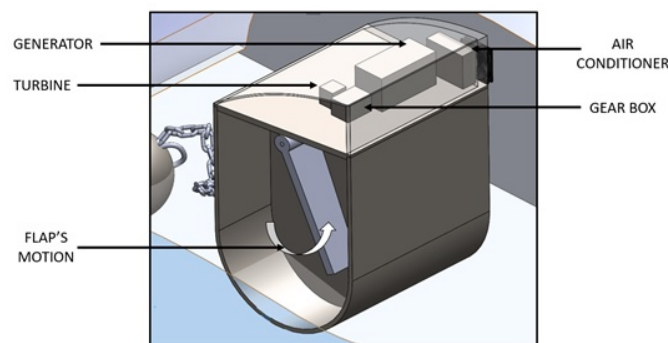


Figure 9: Main components of the device(a)

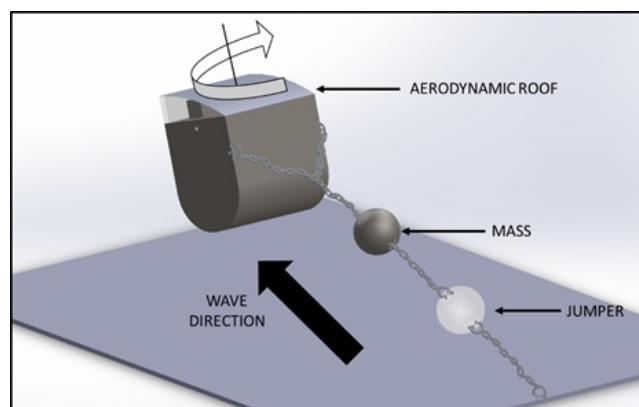


Figure 10: Main components of the device(b)

3.1 Determining physical dimensions

The physical dimensions of the hull reservoir wave energy converter are determined to an extent, which is adequate enough for the preliminary design. The obtained results are to be optimized in the detailed design step. For the calculation of the physical dimensions, the model in [4], is referred. According to [4], ‘Wave Tank Testing of a Pendulum Wave Energy Converter’, The wave height and the wave period of the simulation is set as 3.5 m and 2.2 s. Using these parameters, the wavelength is calculated using the equation below,

$$\lambda = T(gH)^{\frac{1}{2}}$$

Where, $T = 2.2$, $H = 3.5m$ and $g = 9.81ms^{-2}$ Therefore,

$$\lambda = 12m$$

In the preliminary design, the focus is on an application in the off shore and the sea depth (H_R) is about 20 m and the wave period (T_R) is taken as 12 s. At this seas condition which is an intermediate one, the following equation is used to calculate the wave length.

$$\left(\frac{2\pi}{T}\right)^2 = \frac{2\pi g}{\lambda} \tanh\left(\frac{2\pi h}{\lambda}\right)$$

By solving the equation by MATLAB as shown in appendix B, substituting $h = 20$ m and $T = 12s$, the wavelength value was obtained as 118.34m (λ_R).

The length of the hull has determined in the model as 3m, considering a criterion to compromise between using the maximum slope of the waves and reducing the floater size and costs, maximizing the performances of the system. This proportionality of the length of the hull and the wavelength is used to calculate the length of the hull in the real application as shown below. Using the data in table 2 L_R can be calculated

$$\frac{\lambda}{L} = \frac{\lambda_R}{L_R}$$

$$L_R = 28m$$

Symbol	Description	Value
L	Length of the hull of the model	3m
L_R	Length of the hull of the real device	-
λ	Wavelength of the model	13m
λ_R	Wavelength of the real application	118.34m

Table 2: Values of real and model instances

Since the length of the hull is known, other dimensions can be assumed accordingly as shown in figure 11.

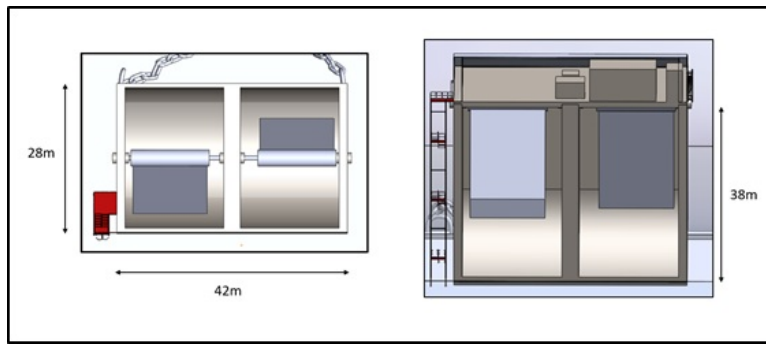
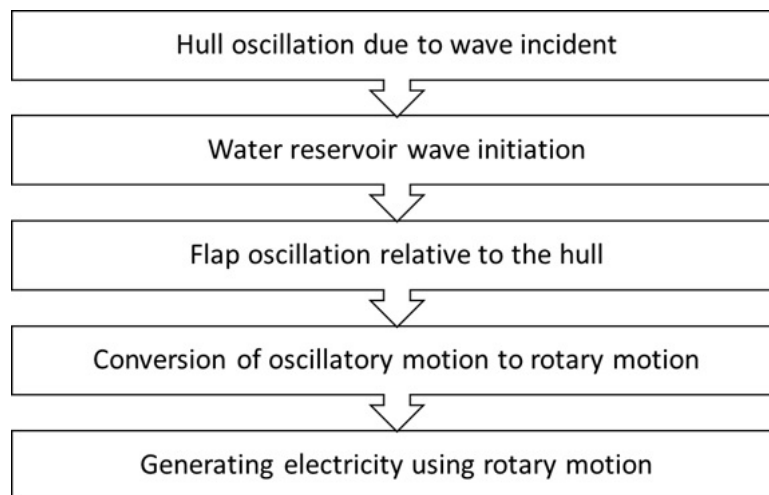


Figure 11: Dimensions of the device

3.2 Development of the mechanisms

The main mechanism of the hull reservoir wave energy converter is the wave energy conversion to electrical energy. This is basically being done using flaps, and a generator. The steps involved in the conversion is shown in the diagram below.



The conversion of oscillatory motion to rotary motion has to be given a special focus, since other energy transmission processes are either natural or widely used in mechanical applications for a longer period of time. Therefore, two options are proposed and the pros and cons of each option has to be considered when choosing the best one for the particular application. The two methods of energy transmitting are,

- A gear mechanism
- Hydraulic pump

3.2.1 Hydraulic pump

A concept of Dr. T. Watabe of an axial piston pump [2] can be used to turn the generator. This setup consists of a oscillating shaft three piston pumps, one speed-up gear, an accumulator and a piston motor. Figure 12 shows how the energy is transmitted.

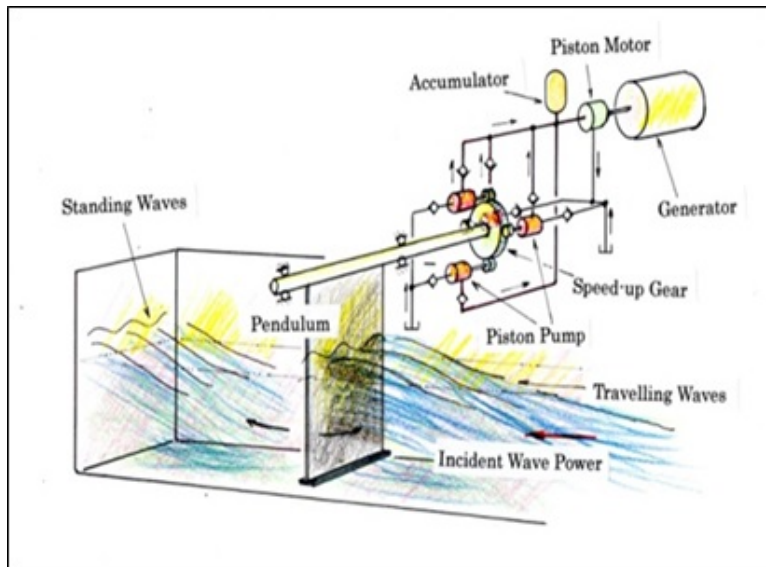


Figure 12: Hydraulic pump concept

There are axial and geared piston pump sets that can be used as shown in figures 13 and 14.

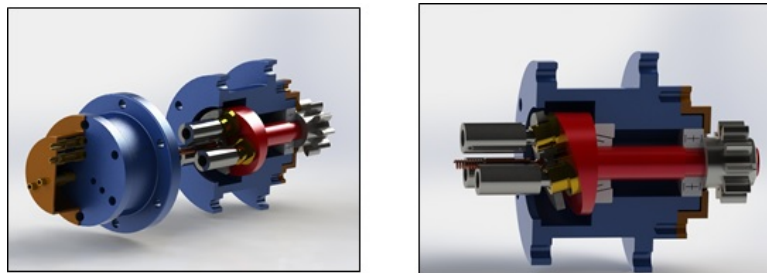


Figure 13: Axial pump unit

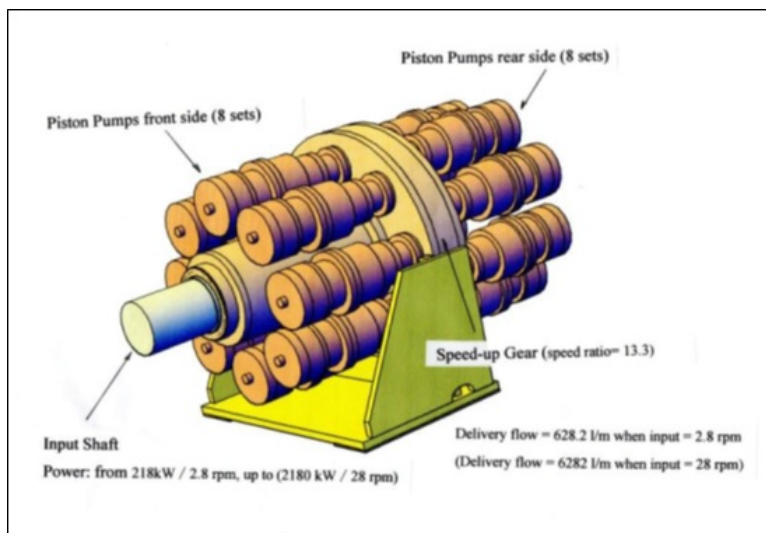


Figure 14: Geared piston pump set

3.2.2 Gear mechanism

As the second option a new gear mechanism was innovated to smoothly transmit oscillatory motion to rotary motion of both flaps of the device and combine them to get the resultant power output.

However, there are possible drawbacks like, the efficiency might not be as good as the hydraulic pump due to moving and contacting metal parts in the gear mechanism and significant amount of energy is needed to initiate the rotation at the beginning. The main mechanism to convert oscillatory motion to rotary motion has three bevel gears and a ratchet mechanism. Here, the ratchet gear is locked with the oscillating shaft but the bevel gears aren't. A pawl in the ratchet mechanism is used to lock the rotation of a bevel gear in one direction as shown in figure 15. The pawls are placed and connected such that the rotation in both directions are ensured as shown in figure 16. As shown in figure 16, when the shaft

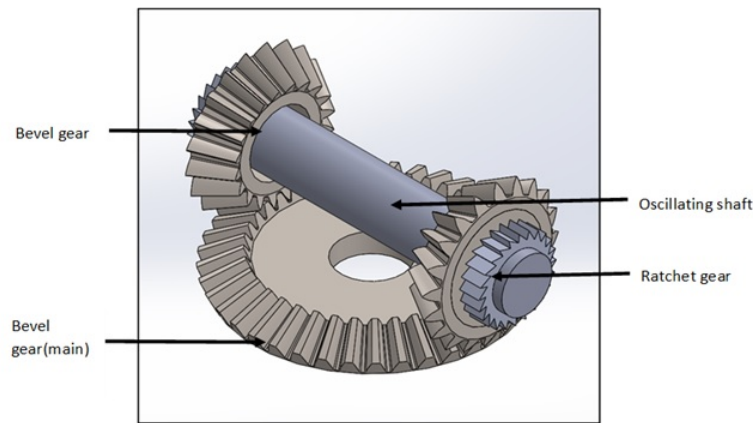


Figure 15: Gear orientation

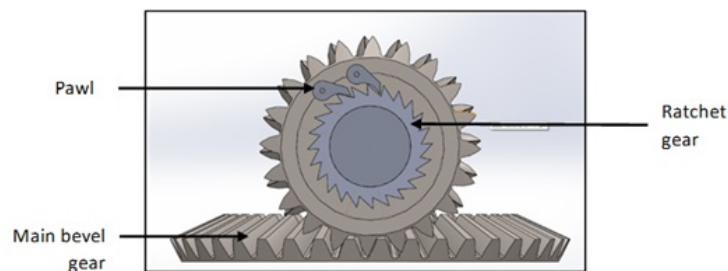


Figure 16: Ratchet mechanism

rotates in the clockwise direction, ratchet gear moves freely. But when it comes to anti-clockwise direction, the gear teeth of ratchet gear contacts with the pawl, which is connected with the bevel gear and initiate the bevel gear's movement in anti-clockwise direction. By using this mechanism for both sides the continuous motion in one direction (in this case anti-clockwise direction) in the main bevel gear is achieved. Since the device consists with double chamber design, it includes two flaps, which are working separately. Therefore, the oscillations of both flaps are integrated to the system as shown in figure 17. The ratchet gears of both mechanisms are connected such that the output rotation is in the same way. Some of the advantages in this design are,

- One generator is adequate for the operation
- Saves the material
- Saves the space of the power house

But some of the problems as, shaft distortion due to speed variation of the two mechanisms and transmitting energy from one flap to another, instead of transmitting energy to the generator might occur. In order to reduce them, coupling of two mechanisms using a internal gear can be used as shown in the figure 18.

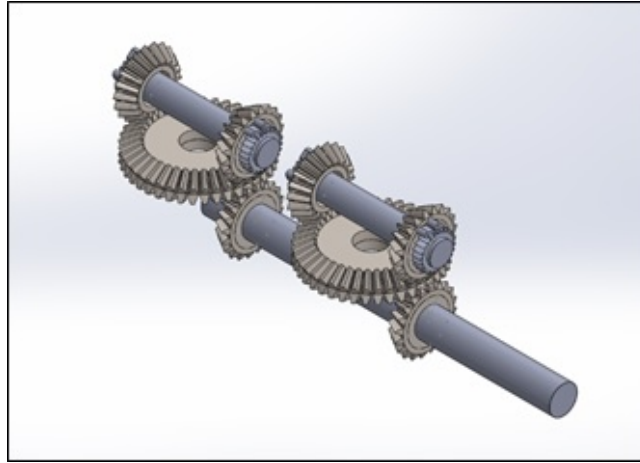


Figure 17: Configuration for double flap design

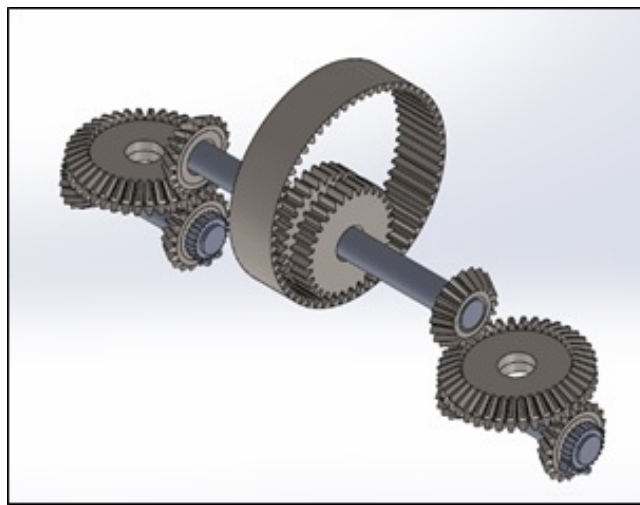


Figure 18: Gear mechanism with the internal gear

This setup minimizes the energy loss since, the internal gear, which is connected with the generator, using a belt works as a energy storage, helps the rotation of the flaps, whenever it lacks the amount of energy given by the waves. On the other hand, shaft distortions won't occur.

3.3 Special Features

3.3.1 Aerodynamic roof

There are two main forces acting upon the device give its rotation and linear movement and those are the sea wave force and wind force. But sea wave force is the dominant force, which is mainly responsible for the pitching movement of the device and the wind force acts as a resistance force for the movement, since it gives a clockwise moment, while the sea wave force tries to rotate it in the anti-clockwise direction. Therefore, in order to lower the magnitude of the wind force, the roof top of the device is designed as shown in the figure 19.

3.3.2 Double chamber design

By using the double chamber design, we try to avoid catastrophic situations that might occur due to excessive rolling in extreme wave conditions. If the water mass inside the hull reservoir acts as one mass due to one chamber design, when rolling happens, the water mass moves to one side of the hull

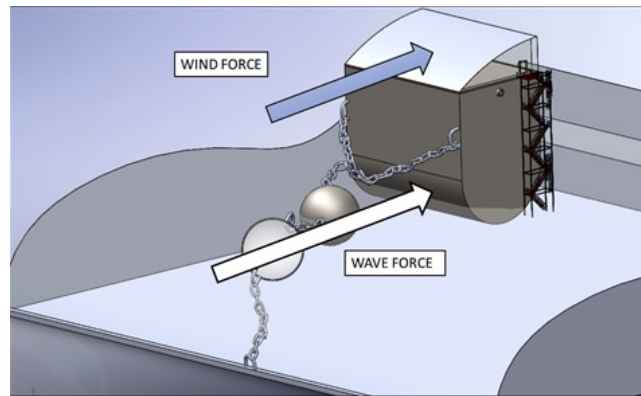


Figure 19: Forces acting on the device

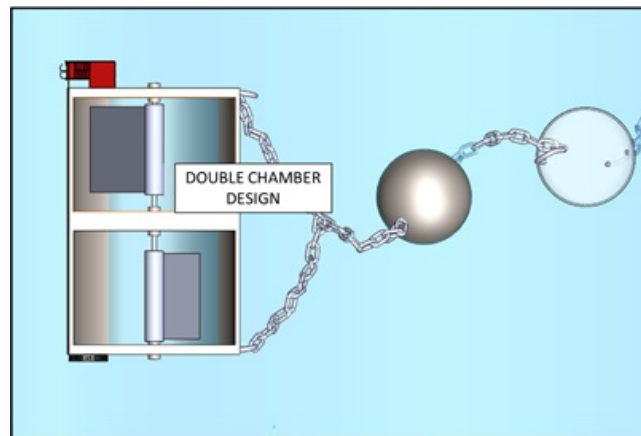


Figure 20: Double chamber design

creating an imbalance of the device. Once another wall between the side walls is implemented, the water, which moves side by side gets blocked at the middle and lower the risk of excessive rolling.

3.4 Safety precautions

1. Usage of belts and lanyards

When doing maintenance work at higher places like vertical walls, workers should use belts and lanyards systems attached to their bodies like in figure 21 in order to reach those places. But since the hull is oscillating with the waves workers can easily loose balance even when they are working on horizontal floors. Therefore they should use safety belts and lanyards at all times, even on horizontal floors. In order to connect the lanyards the hull should be designed with necessary hinges.



Figure 21: Safety belts and lanyards

2. Fences around units

Implementing bar fences around units such as pumps and generators can help in many ways. It restricts accidental contacts with the devices. And also during maintenance instances workers can connect their belts and lanyards to the fence so that they can maintain steady working position to minimize accidents. The figure 2 is an applicable safety fence that can be used as described above.

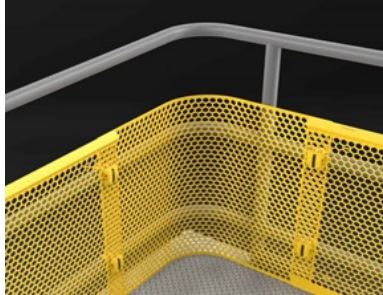


Figure 22: Safety fence that can be used around subunits.

3. Always use reliable lighting

Another thing about working at sea is that it's often very dark. When a sudden storm hits, anytime the sun goes down it can get dark quickly. Darkness makes users more prone to accidents. That's why reliable lighting is so important, especially in low or confined areas. The figure 23 shows a good lighting set up at an offshore working environment. Installing easy-to-see, easy-to-use lighting with customized safety signage helps everyone do their jobs better and warns them of potential hazards.



Figure 23: Good lighting at an offshore working environment

4. Keep work surfaces slip-proof

As the working environment is constantly moving, one can easily slip on the floor. So if the floor itself is slippery it will lead to definite accidents. Therefore the floors should be made slip-proof in the first place. This can be done by steel grating flooring or traction tread flooring as shown in figures 24 and 25 respectively. Even though the floor is good, slip resistant boots should be used to get the maximum use of it. There can be accidentally spilled oils or other lubricants on the floor. So the maintenance crew must clean such places as soon as they can to reduce future accidents.



Figure 24: Steel grating flooring

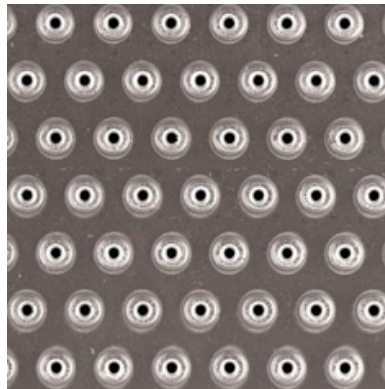


Figure 25: Traction tread flooring

5. Having emergency alarms and lights.

Since the hull is quite a large device it is better to have emergency alarms and light systems at different places. Sometimes crew members can face serious accidents and they might have to call for help immediately. If not there can be severe malfunctioning of devices that need immediate attention or there can be instances like fires. In such cases emergency alarms and lights can instantly aware the whole crew about the situation giving visual and audible signals.



Figure 26: An offshore emergency alarm/ unit

6. Specified path ways with fences.

The upper floor of the hull is a large rectangular area with all sub-units such as generators, power units and pump houses. The crew members have to reach those places frequently for inspections and repairs. But here walking on this open area is very dangerous because the hull is constantly in motion with large oscillations. Therefore it is not a usual open area in land. So one can easily get carried away with the unbalance of the floor and may get fatal accidents. In order to overcome this issue there should be specific walking paths with fences on both sides as

shown in the diagram below. So the members can attach their lanyards to the fences even when walking to minimize risks due to the moving floor.



Figure 27: Specific pathways with safety fences.

7. Emergency getaways.

There can be unstoppable fire raised. Since the number one priority is human lives, there might be an instance where the crew has to evacuate the place immediately. In such cases it's vital to have necessary safety precautions. Implementing safety boats and emergency exits in the design can overcome this issue to a greater extent. The figure 28 is a special life boat used at offshore buildings.



Figure 28: Emergency lifeboats used at offshore buildings.

3.5 Possible problems

1. Noise

The hull is constantly in oscillatory motion. There are many places where water hits the solids parts of the hull. So as a result, a huge noise may arise. The inside of the hull is half filled with water and the water constantly hits the two flaps and inside walls of the hull. The power plant is consisted with a gear box. In the gear box there is a ratchet mechanism used. There can be a high noise due to the operation of the ratchet. So with the addition of sound of other mechanical parts, the inside of the hull and outside gets high noise levels. Use of fabric panels around such devices is a good solution for this. Furthermore office walls can also be fabric paneled and they can be designed as far as away from high noise areas so they are ergonomically suitable to work with.

2. Corrosion

Corrosion is one of the major problems that arise in the device. Contact of water with metals accelerates the corrosion process. It can be minimized up to some level by implementing the device at cold water. So it can be considered as a site selecting criteria. In order to minimize corrosion all pipelines should be galvanized. Anodic and cathodic protections can be used at

required places to protect vital components. Making of complex geometries with non resistive materials can be very expensive. Therefore they can be made using cheaper metals and then apply corrosion preventing coatings. The device is consisted with a pump house to pump sea water in to the hull. So when selecting the pump special high quality sea water corrosion resistant pumps should be used.

3.6 Materials used

Major part of the device that has to be considered when selecting materials is the hull body. When selecting materials, one of the major criteria to be considered is that the hull should weigh less in order to increase the amplitude of oscillations. Another major criterion is that the material should be highly corrosion resistant as it is always in contact with sea water. When selecting materials fiber glass, stainless steel and aluminum were considered as candidates. When considering the corrosion factor, all three candidates are suitable as they are all corrosion resistant. When considering weight factor, stainless steel weighs significantly more when compared with aluminum and fiber glass. Out of aluminum and fiber glass, aluminum weigh less and it is the most durable from all three candidates. Therefore the maintenance costs will be reduced. Stainless steel with reinforcement is selected as the material for the upper floor of the hull because using aluminum for such a place would be not economically suitable. Concrete with reinforcements can also be considered as this is a horizontal floor plus concrete is cheaper. But concrete weigh more in significant amounts and it can shift the center of gravity up leading to unbalance in the hull.

4 Obtaining equations of motion for the device using rigid body equations

One of the problems that is present in the model simulated above is that the motion is only in one plane and so only the motion in the steady state conditions when wave forces come from a single direction can be simulated. In order to simulate the motion considering the sway, roll and yaw motions as well, equations of motion was derived using rigid body equations and as a start, the mathematical model was created to have the same degrees of freedom as [4] so that the results can be compared for the verification. The derivation of the equations is given in appendix C. The equations of motion derived are,

$$\begin{aligned}\dot{X} &= A^{-1}F \\ R_f &= R_1(\alpha) \\ R_0 &= R_1(\theta) \\ R &= R_0R_f\end{aligned}$$

Where,

$$A = \begin{bmatrix} (M+m)\mathbf{I}_{3 \times 3} & m(R\hat{\mathbf{e}}_1 l_f - R_0\hat{\mathbf{e}}_1 l_h) & mR\hat{\mathbf{e}}_1 l_f & \mathbf{0}_{3 \times 3} & \mathbf{0}_{3 \times 1} & \mathbf{0}_{3 \times 1} \\ -M\mathbf{e}_1^T R_f^T \hat{l}_h R_0^T & \mathbf{e}_1^T R_f^T \mathbb{I}_0 \mathbf{e}_1 & 0 & \mathbf{0}_{1 \times 3} & 0 & 0 \\ m\mathbf{e}_1^T \hat{l}_f R^T & \mathbf{e}_1^T (\tilde{\mathbb{I}} \mathbf{e}_1 + m\hat{l}_f R_f^T \hat{\mathbf{e}}_1 l_h) & \mathbf{e}_1^T \tilde{\mathbb{I}} \mathbf{e}_1 & \mathbf{0}_{1 \times 3} & 0 & 0 \\ \mathbf{0}_{3 \times 3} & \mathbf{0}_{3 \times 1} & \mathbf{0}_{3 \times 1} & \mathbf{I}_{3 \times 3} & \mathbf{0}_{3 \times 1} & \mathbf{0}_{3 \times 1} \\ \mathbf{0}_{1 \times 3} & 0 & 0 & \mathbf{0}_{1 \times 3} & 1 & 0 \\ \mathbf{0}_{1 \times 3} & 0 & 0 & \mathbf{0}_{1 \times 3} & 0 & 1 \end{bmatrix}$$

and,

$$F = \begin{bmatrix} (M+m)g\mathbf{e}_3 + m(R_0\hat{\mathbf{e}}_1^2 l_h \omega_0^2 - R\hat{\mathbf{e}}_1^2 l_f (\omega + \omega_0)^2) + f_e \\ \mathbf{e}_1^T R_f^T [\omega_0^2 \mathbb{I}_0 \mathbf{e}_1 \times \mathbf{e}_1 + T_e - l_h \times R_0^T (Mg\mathbf{e}_3 + f_e)] + k_{pto} \omega \\ \mathbf{e}_1^T [(\omega + \omega_0)^2 \tilde{\mathbb{I}} \mathbf{e}_1 \times \mathbf{e}_1 + m l_f \times (R^T g\mathbf{e}_3 + R_f^T \hat{\mathbf{e}}_1 l_h \omega_0)] - k_{pto} \omega \\ v \\ \omega_0 \\ \omega \end{bmatrix}$$

The terms used are defined in C and the solution for the equation is X where,

$$X = [v \quad \omega_0 \quad \omega \quad O \quad \theta \quad \alpha]^T$$

here, O is the position of the object as a vector and θ and α are the pitch of the hull and the angle of the flap relative to the hull respectively. This can also be solved using the Euler's method given in A.1

5 Results

By simulating the equations in section 4 using the MATLAB code in appendix A.2, a set of data for the surge, heave, pitch and flap angle can be obtained for different wave time periods. Then in order to find the resonant frequencies of the device, the maximum amplitude of the results obtained for a certain time period were plotted with the wave time period. The data obtained are shown in figures 29,30,31,32,33,34,35 and 36

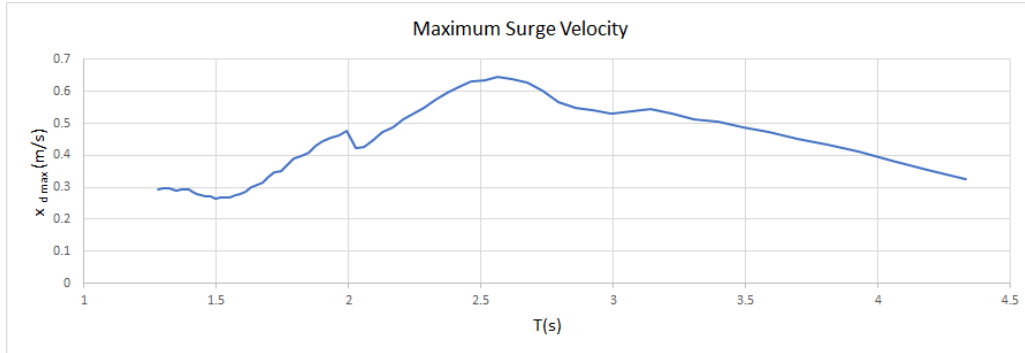


Figure 29: Surge velocity variation with wave time period

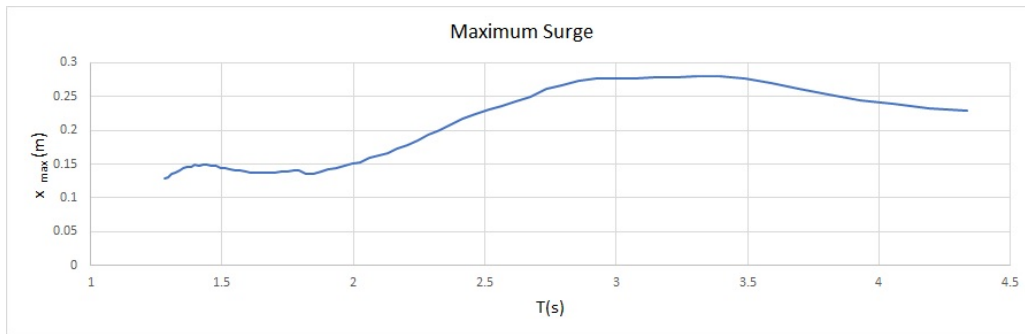


Figure 30: Surge variation with wave time period

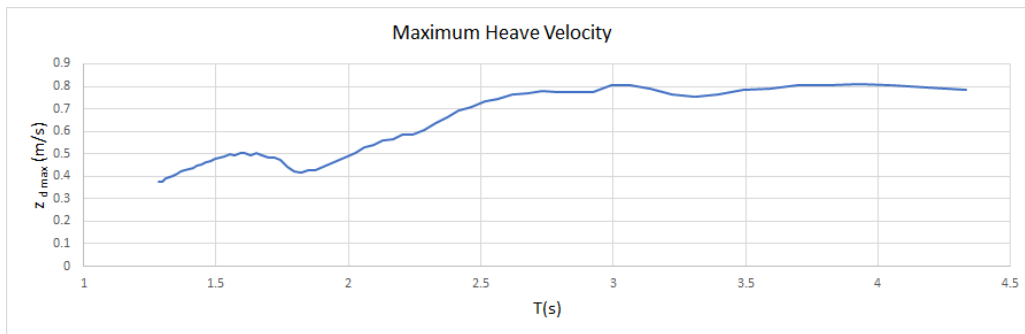


Figure 31: Heave velocity variation with wave time period

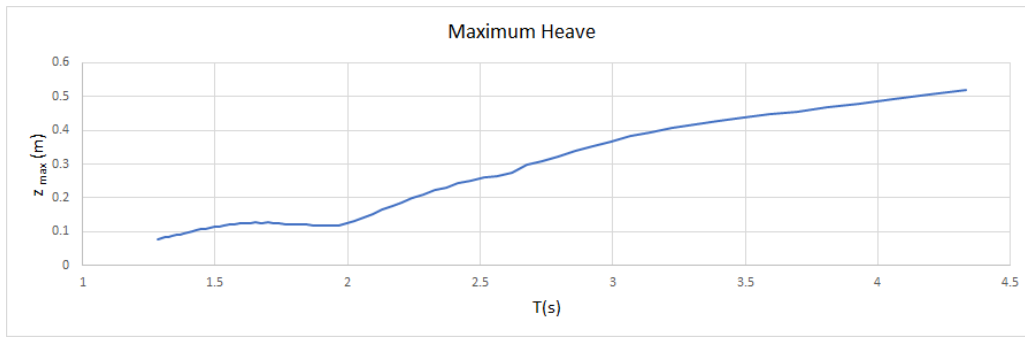


Figure 32: Heave variation with wave time period

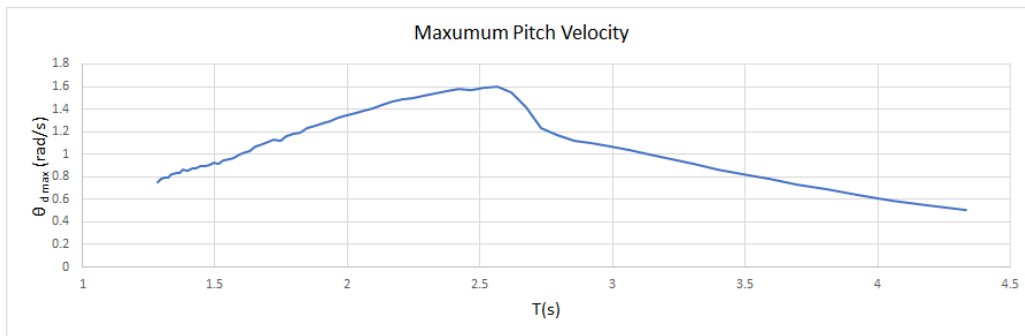


Figure 33: Pitch velocity variation with wave time period

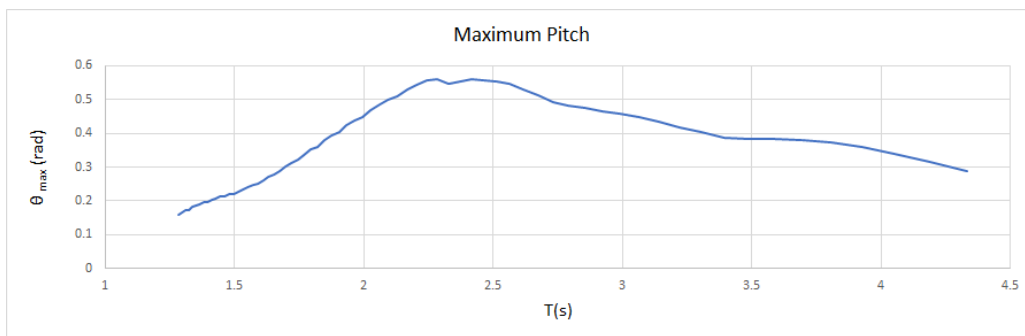


Figure 34: Pitch variation with wave time period

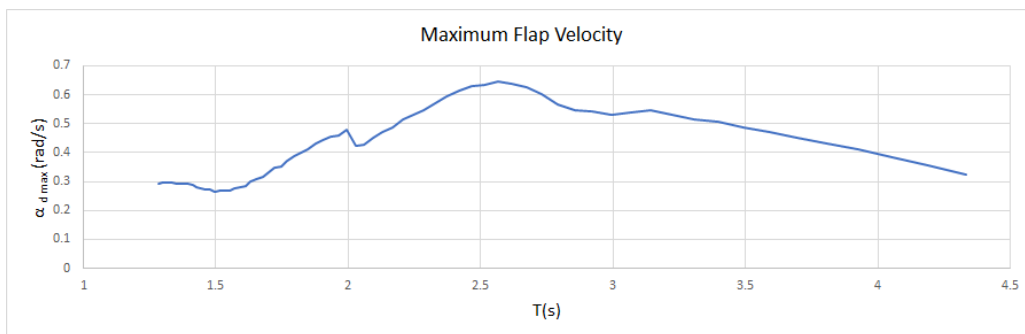


Figure 35: Flap velocity variation with wave time period

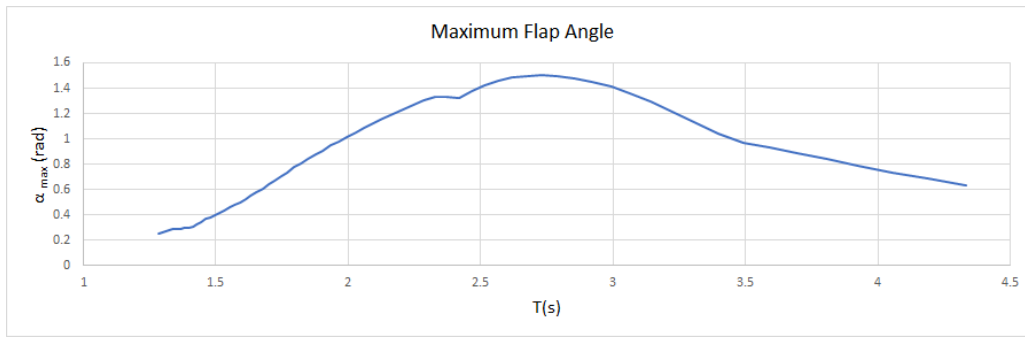


Figure 36: Flap angle variation with wave time period

Therefore it can be seen that the heave and surge displacements are not drastically affected by the wave time period but all the other values maximize between the time periods 1.8s and 2.8. The reason for the values to maximize in this region is because the natural frequency of the model is within this range. to further examine whether resonance occurs within this time figure consider 37 which shows the variation of flap angle α within a time of 10s for different values of time period and it can be seen that for 2.7s time period maximum amplitude occurs and the motion is more uniform.

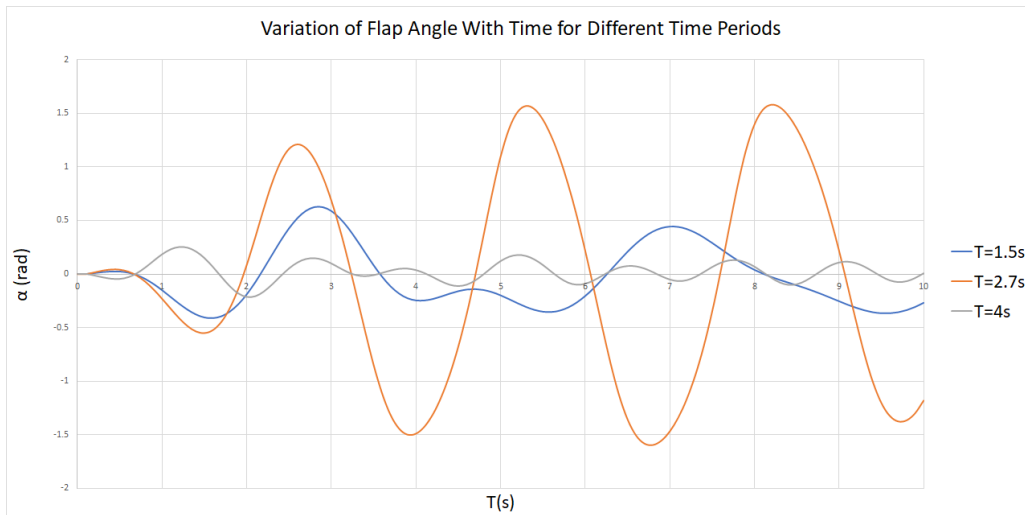


Figure 37: Variation of Flap Angle With Time for Different Time Periods

Since resonance occurs within the time periods 1.8s and 2.8s the variation of the variables were further examined with varying damping constant c this is shown in figures 38,39,40,41,42,43,44 and 45

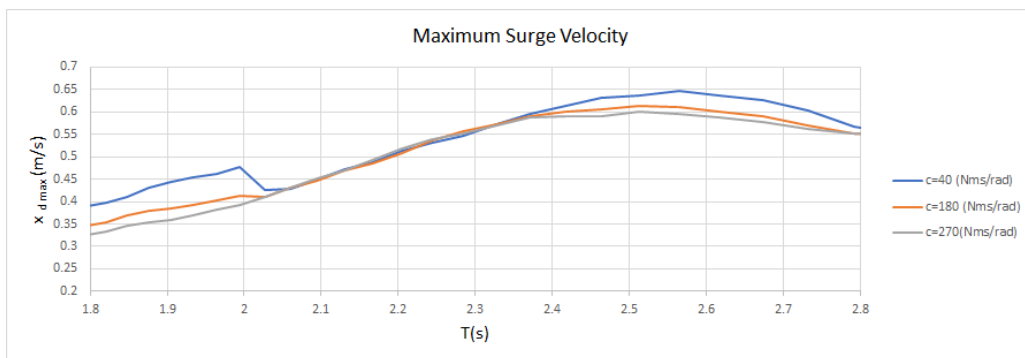


Figure 38: Surge velocity variation with wave time period

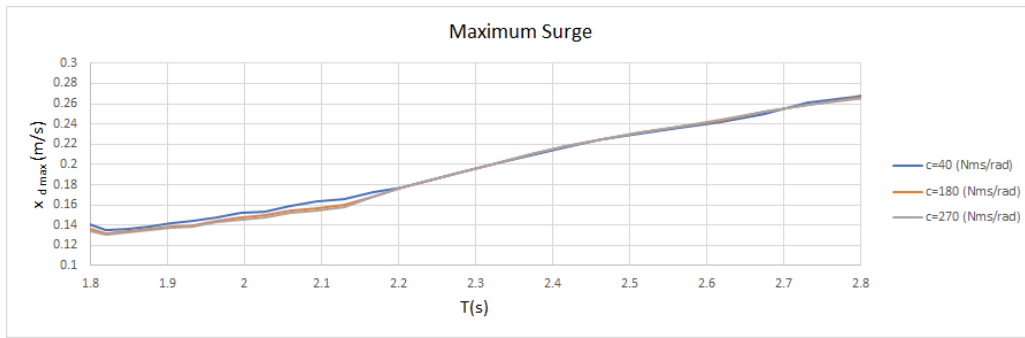


Figure 39: Surge variation with wave time period

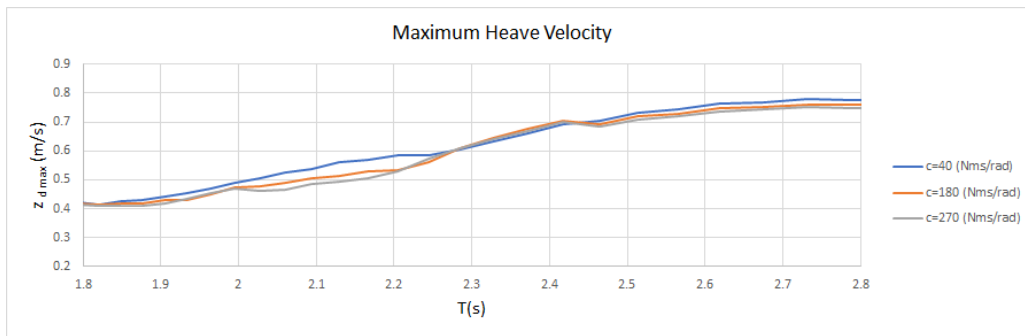


Figure 40: Heave velocity variation with wave time period

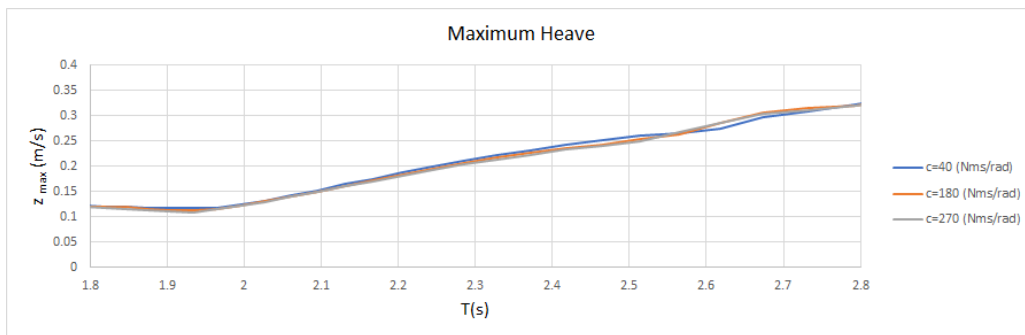


Figure 41: Heave variation with wave time period

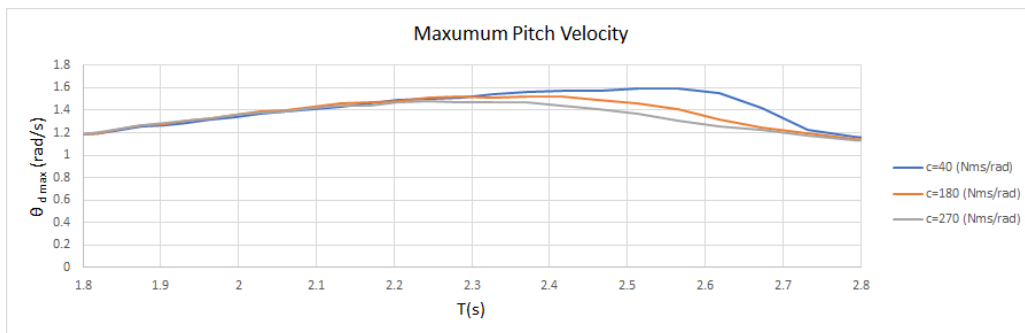


Figure 42: Pitch velocity variation with wave time period

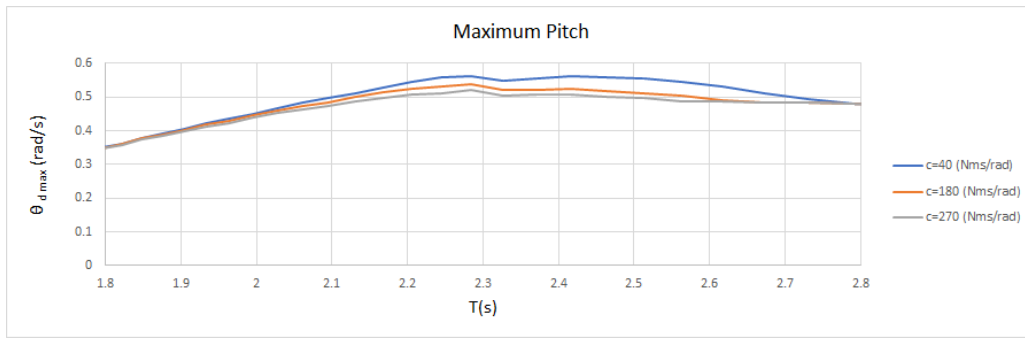


Figure 43: Pitch variation with wave time period

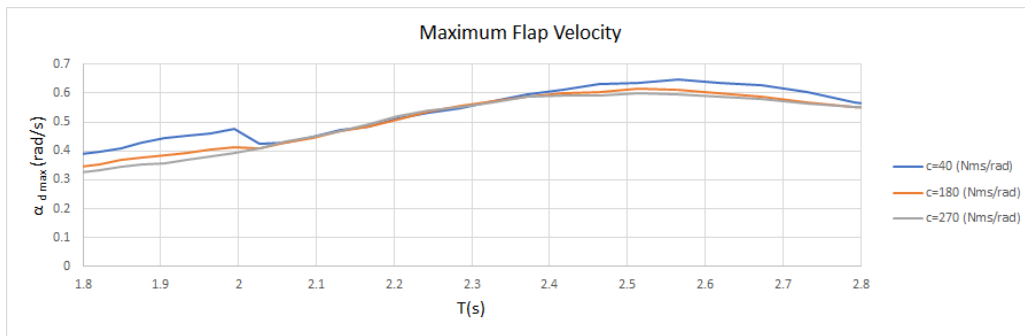


Figure 44: Flap velocity variation with wave time period

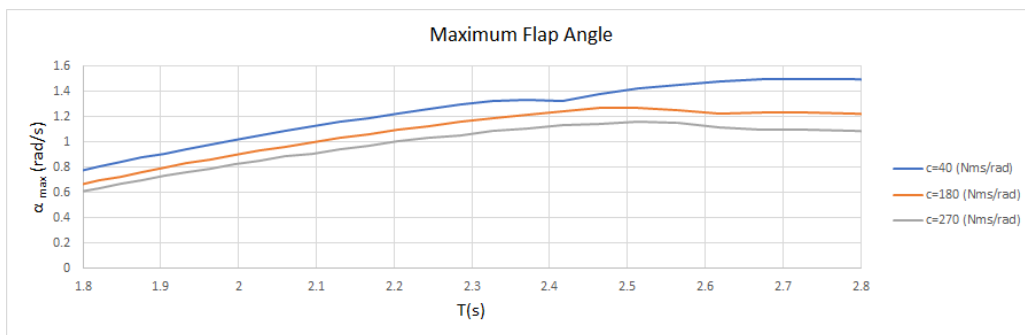


Figure 45: Flap angle variation with wave time period

Also, then average power output that can be calculated using the above values as in figure 46 considering that the maximum values obtained represent the amplitude of the angles θ and α

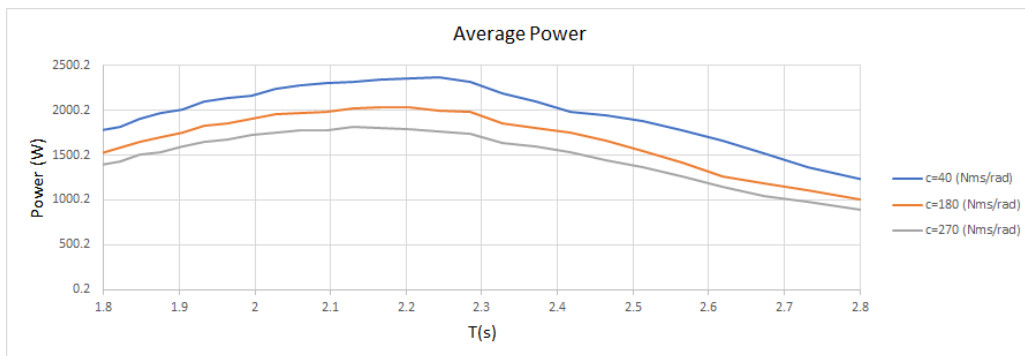


Figure 46: Power variation with wave time period

6 Conclusion

One of the objectives of this project was to model the dynamics of the HRWEC using the equations of motion given in [4] and using a separate set of hydrodynamic data that has been obtained using a software and try and match the results obtained in [4]. The figures 47 and 48 show the data obtained in [4] and when comparing figure 47 with with figures 39,41,43 and figure 48 with figures 38,40,42, it can be seen that although there is no perfect match, the time periods at which the maximum and minimum values are reached is similar. But there is a difference in the magnitudes of the values and this is most probably because of the damping matrices that was used to prevent the model from reaching unrealistic and large values during simulation (D') matrix. Hence it is clear that the simulation data is reliable up to a certain extent.

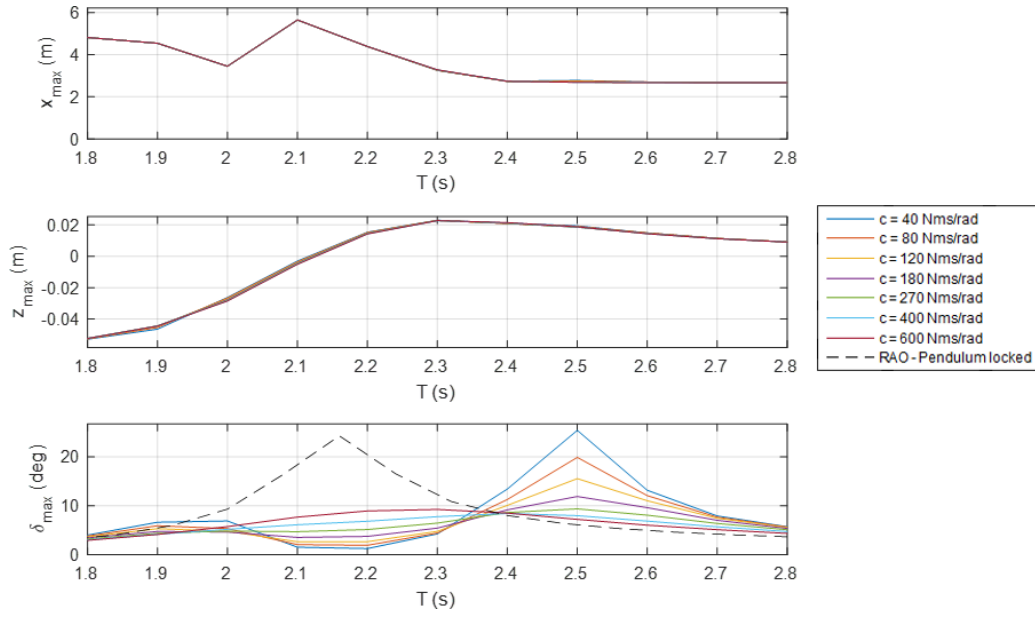


Figure 47: Surge, heave and pitch velocity variation of the hull with time period

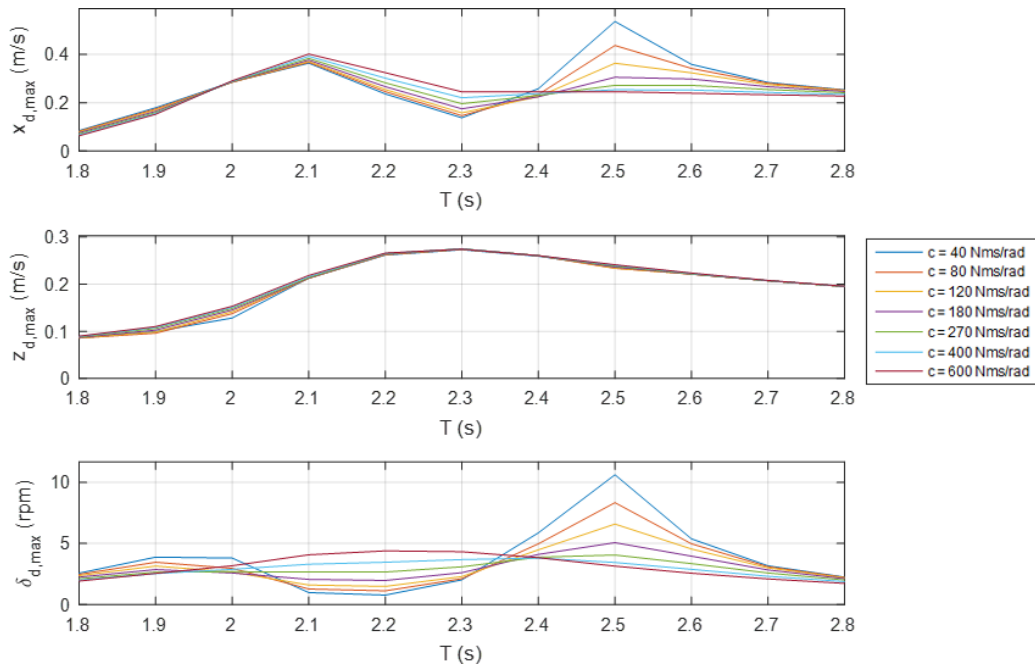


Figure 48: Surge, heave and pitch velocity variation of the hull with time period

From figure 46 it is clear that the maximum power is obtained at around $2.2s$ and the time period range from about $2.1s$ to $2.5s$ also have satisfactory results. A similar conclusion has been reached in [4] as well. Therefore these results can be obtained in determining the most suitable dimensions of the WEC as done in section 3.1.

The equations obtained in appendix C must be modified so that it would have 6 degrees of freedom to the hull and 1 degree of freedom for the flap so that the complete motion of the device can be described which can help to gain more accurate and realistic results.

7 Future Work

The future goals of the project is to

1. Simulate the device after adding water inside the hull
2. Modify the equations in section 4 to have more degrees of freedom
3. Further development of the preliminary model
4. Design, fabrication and testing of an experimental model

Acknowledgments

It is with great honor that we express our sincere gratitude to our supervisor Dr.S.D.G.S.P.Gunawardena, Department of Mechanical Engineering for the immense support and guidance given whenever we need. Furthermore, we are very obliged to Mr. Chanaka Bandara of Department of Mechanical engineering, who gave us his time without hesitations, to make this project a success.

Appendix A Mathematical Simulation of the HRWEC

A.1 Euler's method

Consider an first order diffrential equation,

$$A\dot{x} + Bx = F(x)$$

In order to solve the equation to obtain the values of x for different time intervals, the equation must be discretized considering that the gradient of x with respect to time remains constant within a small time interval dt . Then let x be x_k at a certain time which is known and x_{k+1} be x after a time dt which must be determined. Then, x_{k+1} can be found by,

$$A \frac{x_{k+1} - x_k}{dt} + Bx_k = F(x_k)$$
$$x_{k+1} = x_k + dtA^{-1}(F(x_k) - Bx_k)$$

A.2 Matlab Code

```
1 function HRWEC(frequency)
2 dat=load('hydrodynamic_coef.mat');%data for forces from waves
3 wav_freq=frequency;%wavefrequency
4
5 T=5;%simulation time
6 dt=0.1;%time step
7 time=linspace(0,T,(T/dt)+1);%time matrix
8 g=9.81;%acceleration due to gravity
9
10
11 a_0=[0;0];%initial orientation of hull,theta and flap alpha
12 dota_0=[0;0];%initial angular velocity of hull,theta and flap alpha
13 o_0=[0;0;0];%initial position of device
14 doto_0=[0;0;0];%initial velocity of device
15 c=270;%damping constant
16 w=3;%width of the hull
17 r=1.5;%radius of curvature of the hull
18 d=[0;0;0.858];%position of the hinge from the center of mass of
    hull
19 mb=3176;%hull mass
20 Ib=2168;%moment of inertia of the hull about y axis
21 mf=410;%mass of the flap
22 If=88.18;%momet of inertia of the flap about center of gravity
23 l=0.866;%length of the flap
24 a=2*r*w;%cross sectional area
25 density=1000;%density of water
26
27 %mooring system constants
28 ang_moor=deg2rad(10);
29 Pm=[-1*r*sin(ang_moor);0;-1*r*cos(ang_moor)]+d;%position the cable
    is fixed to the hull relativr to its center of gravity
30 %Pm=[-r;0;0]+d;
```

```

31 Fb=250;%net gravity force
32 Fg=98;%net buoyancy force
33 l1=2;%line 1 length
34 l2=0.4;%line 2 length
35 l3=1.8;%line 3 length
36 moor_init=[-3.5,0,-2];%moor anchor point
37 save('moor_init.mat','moor_init')
38 y0=[doto_0(1);doto_0(3);dota_0(1);dota_0(2);o_0(1);o_0(2);a_0(1);
    a_0(2)];%initial coditions
39 amoor=zeros(3,length(time));nmoor=1;%moor data matrix
40 Y=zeros(8,length(time)+1);%hull data matrix
41 Y(:,1)=y0;
42
43 %using euler's method to solve the ODEs
44 for i=1:length(time)
45     fn=ODEeq(time(i),y0);
46     y=y0+dt*fn;
47     Y(:,i+1)=y;
48     y0=y;
49 end
50
51 %plot the motion of the body
52 Xm=Y(5,:);Zm=Y(6,:);Thetam=Y(7,:);Alpham=Y(8,:);Am1=amoor(1,:);Am2=
    amoor(2,:);Am3=amoor(3,:);
53 for i=1:length(time)
54     O=[Xm(i);0;Zm(i)];
55     Theta=Thetam(i);Alpha=Alpham(i);A1=Am1(i);A2=Am2(i);A3=Am3(i);%
        XD=XDm(i);ZD=ZDm(i);
56     R1=[cos(Theta) 0 sin(Theta);0 1 0;-1*sin(Theta) 0 cos(Theta)];%
        rotation of the hull
57     R2=R1*[cos(Alpha) 0 sin(Alpha);0 1 0;-1*sin(Alpha) 0 cos(Alpha)
        ];%rotation of the flap relative to the hull
58     plotf(O,R1,R2,A1,A2,A3)
59     pause(dt);
60
61 end
62
63 %defining the differential equations
64 function dxdt=ODEeq(t,x)%x=[xdot(1);zdot(2);thetadot(3);
    alphasdot(4);x(5);z(6);theta(7);alpha(8)]
65     dottheta=x(3);dotalpha=x(4);
66     theta=x(7);alpha=x(8);
67     Dam=[dat.B11(wav_freq) 0 dat.B15(wav_freq) 0;0 dat.B33(
        wav_freq) 0 0;dat.B51(wav_freq) 0 dat.B55(wav_freq) 0;0
        0 0 0];
68     Mam=[dat.Am11(wav_freq) 0 dat.Am15(wav_freq) 0;0 dat.Am33(
        wav_freq) 0 0;dat.Am51(wav_freq) 0 dat.Am55(wav_freq)
        0;0 0 0 0];
69     Fe=1000*[dat.Fe1(wav_freq)*sin(dat.Omega(wav_freq)*t+
        deg2rad(dat.Fph1(wav_freq)));dat.Fe3(wav_freq)*sin(dat.

```



```

70     Omega( wav_freq)*t+deg2rad( dat . Fph3( wav_freq) ) ); dat . Fe5(
71     wav_freq)*sin( dat . Omega( wav_freq)*t+deg2rad( dat . Fph5(
72     wav_freq) ) ); 0];
73
74 Mhp=[mf+mb 0 0 0;0 mf+mb 0 0;0 0 Ib+If+mf*(d(3)^2+l^2)-2*mf
75     *d(3)*l*cos( alpha ) 0;0 0 0 If+mf*l*l];
76
77 Mc=[0 0 mf*(d(3)*cos( theta)-l*cos( theta+alpha)) -1*mf*l*cos
78     ( theta+alpha );
79     0 0 -1*mf*(d(3)*sin( theta)-l*sin( theta+alpha)) mf*l*sin
80     ( theta+alpha );
81     mf*(d(3)*cos( theta)-l*cos( alpha+theta)) -1*mf*(d(3)*sin
82     ( theta)-l*sin( theta+alpha)) 0 If+mf*l*l-mf*d(3)*l*
83     cos( alpha );
84     -1*mf*l*cos( theta+alpha) mf*l*sin( theta+alpha) If+mf*l*
85     l-mf*d(3)*l*cos( alpha) 0];
86 Ms=Mam+Mhp+Mc;
87 M=[Ms zeros(4,4);zeros(4,4) eye(4)];
88
89 Dpto=[0 0 0 0;0 0 0 0;0 0 0 0;0 0 0 c];
90 cxdot=30000;%hydrodynamic damping due to surge velocity
91 czdot=30000;%hydrodynamic damping due to heave velocity
92 cthetadot=10000;%hydrodynamic damping due to pitching
93     velocity
94 calphadot=400;%damping to represent losses due to flap
95     movement
96 Dhydro=[cxdot 0 0 0;0 czdot 0 0;0 0 cthetadot 0;0 0 0
97     calphadot];
98 D=[Dpto+Dam+Dhydro zeros(4,4);-1*eye(4) zeros(4,4)];
99
100 K=[0;-1*density*g*a*x(6);-1.25*(mf+mb)*g*d(3)*sin( theta)
101     ;0;0;0;0;0];%restoring forces due to hydrodynamic motion
102 Fmoor=solve_equations_moor(x(5),x(6),x(7));
103
104 Fgr=[0;0;-1*mf*g*(d(3)*sin( theta)-l*sin( theta+alpha));mf*g*
105     l*sin( theta+alpha)];
106 Fcor=[mf*(l*( dottheta+dotalpha)^2*sin( theta+alpha)-d(3)*
107     dottheta^2*sin( theta));
108     mf*(l*( dottheta+dotalpha)^2*cos( theta+alpha)-d(3)*
109     dottheta^2*cos( theta));
110     -1*mf*d(3)*l*sin( alpha)*(( dottheta+dotalpha)^2-dottheta
111     ^2);
112     -1*mf*d(3)*l*dottheta^2*sin( alpha)];
113
114 F=[-1*(Fgr+Fcor)+Fe+Fmoor;0;0;0;0]-(D*x)+K;
115 dxdt=M\F;%differential equation

```

```

103     end
104
105
106 %solving the mooring equations
107     function [Fmoor]=solve_equations_moor(ox,oz,thetam)
108         Rm=[cos(thetam) 0 sin(thetam);0 1 0;-1*sin(thetam) 0 cos(
            thetam)];
109         pm(1)=Rm(1,1)*Pm(1)+Rm(1,2)*Pm(2)+Rm(1,3)*Pm(3);
110         pm(2)=Rm(2,1)*Pm(1)+Rm(2,2)*Pm(2)+Rm(2,3)*Pm(3);
111         pm(3)=Rm(3,1)*Pm(1)+Rm(3,2)*Pm(2)+Rm(3,3)*Pm(3);
112         pm0=pm;
113         pm(1)=pm(1)+ox; pm(3)=pm(3)+oz;
114         xd=sqrt((moor_init(1)-pm(1))*(moor_init(1)-pm(1)));
115         zd=sqrt((pm(3)-moor_init(3))*(pm(3)-moor_init(3)));
116         function F=eq_sol(x)%set of equations
117             F(1)=x(3)*cos(x(6))+x(2)*cos(x(5))-Fb;
118             F(2)=x(2)*cos(x(5))+x(1)*cos(x(4))-Fg;
119             F(3)=x(3)*sin(x(6))-x(2)*sin(x(5));
120             F(4)=x(2)*sin(x(5))-x(1)*sin(x(4));
121             F(5)=l3*sin(x(6))+l2*sin(x(5))+l1*sin(x(4))-xd;
122             F(6)=l3*cos(x(6))-l2*cos(x(5))+l1*cos(x(4))-zd;
123         end
124         options=optimset('TolFun',.001,'MaxIter',100000,'
            MaxFunEvals',100000);
125         x=fsolve(@eq_sol,[0 0 0 0 0 0],options);%solve equations
126         Fx=-1*x(1)*sin(x(4));%horizontal force acting on the hull
127         Fz=-1*x(1)*cos(x(4));%vertical force acting on the hull
128         ymoor=[Fx;0;Fz];
129         Tmoor=cross(pm0,ymoor);%torque acting on the hull
130         Fmoor=[Fx;Fz;Tmoor(2);0];%mooring forces
131         amoor(:,nmoor)=[x(4);x(5);x(6)];
132         nmoor=nmoor+1;
133     end
134
135
136 function plotf(o,R1,R2,A1,A2,A3)%plotting the HRWEC and the
    mooring system
137     [Xs,X3,X4,Y1,Y2,Y3,Y4,Zs,Z3,Z4,cs,c3,c4]=object();%create
        object()
138
139     %bring the center of mass to origin to rotate the hull
        about it
140     Zs=Zs+d(3);Z3=Z3+d(3);
141     lg0=zeros(3,1);%position of the hinge after rotation of the
        hull
142
143     %finding the new position of the hinge
144     lg0(1)=R1(1,1)*d(1)+R1(1,2)*d(2)+R1(1,3)*d(3);
145     lg0(2)=R1(2,1)*d(1)+R1(2,2)*d(2)+R1(2,3)*d(3);
146     lg0(3)=R1(3,1)*d(1)+R1(3,2)*d(2)+R1(3,3)*d(3);

```

```

147     lg0=lg0-d;
148
149 %rotate the hull
150 %side1
151 XX1=R1(1,1)*Xs+R1(1,2)*Y1+R1(1,3)*Zs;
152 YY1=R1(2,1)*Xs+R1(2,2)*Y1+R1(2,3)*Zs;
153 ZZ1=R1(3,1)*Xs+R1(3,2)*Y1+R1(3,3)*Zs;
154 %side2
155 XX2=R1(1,1)*Xs+R1(1,2)*Y2+R1(1,3)*Zs;
156 YY2=R1(2,1)*Xs+R1(2,2)*Y2+R1(2,3)*Zs;
157 ZZ2=R1(3,1)*Xs+R1(3,2)*Y2+R1(3,3)*Zs;
158 %bottom
159 XX3=R1(1,1)*X3+R1(1,2)*Y3+R1(1,3)*Z3;
160 YY3=R1(2,1)*X3+R1(2,2)*Y3+R1(2,3)*Z3;
161 ZZ3=R1(3,1)*X3+R1(3,2)*Y3+R1(3,3)*Z3;
162
163 %set the hull back to the original position
164 %ZZ1=ZZ1-d(3);ZZ2=ZZ2-d(3);ZZ3=ZZ3-d(3);
165
166 %rotate flap
167 XX4=R2(1,1)*X4+R2(1,2)*Y4+R2(1,3)*Z4;
168 YY4=R2(2,1)*X4+R2(2,2)*Y4+R2(2,3)*Z4;
169 ZZ4=R2(3,1)*X4+R2(3,2)*Y4+R2(3,3)*Z4;
170
171 %move flap due to the motion of the hinge
172 XX4=XX4+lg0(1);YY4=YY4+lg0(2);ZZ4=ZZ4+lg0(3);
173
174 %move flap to position of hull when centroid is at origin
175 ZZ4=ZZ4+d(3);
176
177 %for linear motion of the system
178 XX1=XX1+o(1);XX2=XX2+o(1);XX3=XX3+o(1);XX4=XX4+o(1);
179 YY1=YY1+o(2);YY2=YY2+o(2);YY3=YY3+o(2);YY4=YY4+o(2);
180 ZZ1=ZZ1+o(3);ZZ2=ZZ2+o(3);ZZ3=ZZ3+o(3);ZZ4=ZZ4+o(3);
181
182
183 %%%%%%%%%%%%%%%%%%%%%%%%%%%%%%%%%%%%%%%%%%%%%%%%%%%%%%%%%%%%%%%%%%%%%%%%%%
184 %mooring system
185 pfx=moor_init(1);
186 pfz=moor_init(3);
187 pax=pfx+l3*sin(A3);
188 paz=pfz+l3*cos(A3);
189 pbx=pax+l2*sin(A2);
190 pbz=paz-l2*cos(A2);
191 pcx=pbx+l1*sin(A1);
192 pcz=pbz+l1*cos(A1);
193 yy=zeros(1,30);
194 x3=linspace(pfx,pax,10);
195 z3=linspace(pfz,paz,10);
196 x2=linspace(pax,pbx,10);

```

```

197     z2=linspace(paz,pbz,10);
198     x1=linspace(pbx,pcx,10);
199     z1=linspace(pbz,pcz,10);
200     xx=[x3 x2 x1];zz=[z3 z2 z1];
201
202     s1=surf(XX1,YY1,ZZ1,cs,'FaceAlpha',0.5);%plot side 1
203     s1.EdgeColor='none';
204     axis([-5 5 -5 5 -5 5]);
205     hold on
206     s2=surf(XX2,YY2,ZZ2,cs,'FaceAlpha',0.5);%plot side 2
207     s2.EdgeColor='none';
208     s3=surf(XX3,YY3,ZZ3,c3,'FaceAlpha',0.5);%plot bottom of the
        hull
209     s3.EdgeColor='none';
210     s4=surf(XX4,YY4,ZZ4,c4);%plot flap
211     s4.EdgeColor='none';
212     xlabel('x');ylabel('y');zlabel('z');
213     plot3(xx,yy,zz,'LineWidth',3,'Color','black')%plot mooring
214     hold off
215 end
216
217 function [Xs,X3,X4,Y1,Y2,Y3,Y4,Zs,Z3,Z4,cs,c3,c4]=object()%
    define the objects
218     div=64;
219     %sides of the hull
220     [angle_curvature,radius]=meshgrid(linspace(0,pi,div),
        linspace(0,r,div));
221     Xs=radius.*cos(angle_curvature);
222     Zs=-radius.*sin(angle_curvature);
223     Y1=(w/2)*ones(div,div);%for side 1
224     Y2=(-w/2)*ones(div,div);%for side 2
225
226     %bottom of the hull
227     [X3,Y3]=meshgrid(linspace(-w/2,w/2,div));
228     Z3=-sqrt(r^2-X3.^2);
229
230     %flap
231     [Y4,Z4]=meshgrid(linspace(-w/2,w/2,div),linspace(0,r,div));
232     X4=zeros(div);
233     Z4=Z4*-1;
234
235     %colour of sides
236     cs(:, :, 1)=0*ones(div,div);
237     cs(:, :, 2)=1*ones(div,div);
238     cs(:, :, 3)=0*ones(div,div);
239
240     %colour of bottom of the hull
241     c3(:, :, 1)=0*ones(div,div);
242     c3(:, :, 2)=0*ones(div,div);
243     c3(:, :, 3)=1*ones(div,div);

```

```
244
245     %colour of flap
246     c4 (:,:,1)=1*ones(div,div);
247     c4 (:,:,2)=0*ones(div,div);
248     c4 (:,:,3)=0*ones(div,div);
249 end
250 end
```

Appendix B Sea wavelength calculation

The wavelength of intermediate depths is given by the equation

$$\left(\frac{2\pi}{T}\right)^2 = \frac{2\pi g}{\lambda} \tanh\left(\frac{2\pi h}{\lambda}\right)$$

The wavelength λ can be determined if the time period of the wave, T , and the wave depth, h are known. since this equation is not possible to be solved analytically, it was solved using MATLAB. The code used is shown below.

```
1 function Lambda()
2     function F=eq_sol(x)
3         F=((2*pi/12)^2)-(2*pi*9.81*tanh(2*pi*20/x))/x ;
4     end
5     options=optimset('TolFun',.001,'MaxIter',100000,'
        MaxFunEvals',100000);
6     x=fsolve(@eq_sol,[0.8],options);
7     x
8 end
```

Appendix C Derivation of the equations of motion

The object of focus here consist of a hull with a flap pivoted to it so that it has the freedom to rotate about one axis relative to the hull. The Figure 49 shows this object when the hull is rotated by an angle θ and the flap by an angle α relative to the hull. Let the inertial frame of reference be \mathbf{e} and

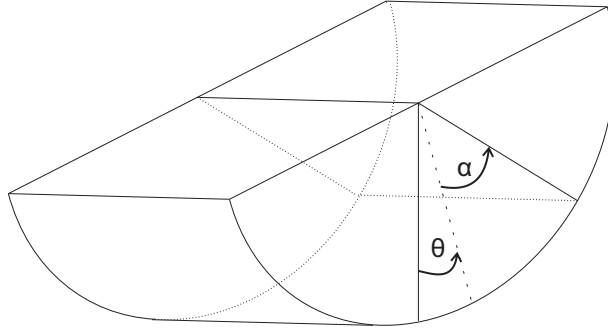


Figure 49: Model of the device

the frame parallel to the inertial frame of reference fixed to the center of mass of the hull, O be \mathbf{e}' . Therefore, O is the position of the center of mass of the hull relative to the inertial frame of reference. Also let the frame relative to the hull fixed to the center of mass be \mathbf{b}_0 . Then let the position of the pivot point of the flap relative to \mathbf{b}_0 be $-l_h$ and the frame parallel to \mathbf{b}_0 fixed at the pivot point be \mathbf{b}_0' . Then the position of the center of mass relative to \mathbf{b}_0' , will be l_h . Let the frame parallel to the flap fixed to the pivot point be \mathbf{b}' and the position of the center of mass of the flap relative to \mathbf{b}' be l_f then the frame fixed to the center of mass of the flap can be taken as \mathbf{b} . Also the mass of the hull and flap be M & m respectively and the inertia tensors of them be \mathbb{I}_0 and \mathbb{I}_f . Here, \mathbb{I}_0 is defined with respect to frame \mathbf{b}_0 and \mathbb{I} relative to frame \mathbf{b} . Figure 50 shows the frames that are taken. If the distance from the center of mass of hull to the pivot point is l^h and the distance from the center of mass of the flap to the pivot point is l^f where they are positive numbers,

$$l_h = \begin{bmatrix} 0 \\ 0 \\ -l^h \end{bmatrix}, l_f = \begin{bmatrix} 0 \\ 0 \\ -l^f \end{bmatrix}$$

Here the motion of the whole body can be assumed to be only sway, heave and pitch motions therefore the frames \mathbf{b}_0 and \mathbf{b}' can be defined as,

$$\begin{aligned} \mathbf{b}_0 &= \mathbf{e}' R_1(\theta) \\ \mathbf{b}' &= \mathbf{b}_0' R_1(\alpha) \end{aligned}$$

Therefore, if $R_1(\theta) = R_0$, $R_1(\alpha) = R_f$ and $R_1(\theta)R_1(\alpha) = R$,

$$\begin{aligned} \mathbf{b}_0 &= \mathbf{e} R_1(\theta) \\ \mathbf{b}_0 &= \mathbf{e} R_0 \\ \mathbf{b} &= \mathbf{e} R_1(\theta) R_1(\alpha) \\ \mathbf{b} &= \mathbf{e} R_0 R_f \\ \mathbf{b} &= \mathbf{e} R \end{aligned}$$

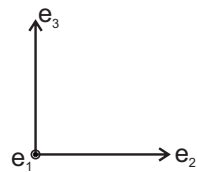


Figure 50: Frames of reference

Where,

$$R_1(\theta) = \begin{bmatrix} 1 & 0 & 0 \\ 0 & \cos \theta & -\sin \theta \\ 0 & \sin \theta & \cos \theta \end{bmatrix}, R_1(\alpha) = \begin{bmatrix} 1 & 0 & 0 \\ 0 & \cos \alpha & -\sin \alpha \\ 0 & \sin \alpha & \cos \alpha \end{bmatrix}$$

Here, θ is the pitch angle of the hull relative to the inertial frame and α is the pitch angle of the flap relative to the hull. Then the body angular velocities of the hull, Ω_0 and the flap, Ω can be defined as,

$$\begin{aligned}\Omega_0 &= \begin{bmatrix} \dot{\theta} \\ 0 \\ 0 \end{bmatrix} \\ \Omega_0 &= \dot{\theta} \mathbf{e}_1 \\ \Omega &= R_1^T(\alpha) \Omega_0 + \begin{bmatrix} \dot{\alpha} \\ 0 \\ 0 \end{bmatrix} \\ \Omega &= \begin{bmatrix} 1 & 0 & 0 \\ 0 & \cos \alpha & \sin \alpha \\ 0 & -\sin \alpha & \cos \alpha \end{bmatrix} \begin{bmatrix} \dot{\theta} \\ 0 \\ 0 \end{bmatrix} + \begin{bmatrix} \dot{\alpha} \\ 0 \\ 0 \end{bmatrix} \\ \Omega &= \begin{bmatrix} \dot{\theta} + \dot{\alpha} \\ 0 \\ 0 \end{bmatrix} \\ \Omega &= (\dot{\theta} + \dot{\alpha}) \mathbf{e}_1\end{aligned}$$

Forces acting on the system

Let the torque acting on the flap at the pivot point be T_p relative to the \mathbf{b}' frame where,

$$T_p = \begin{bmatrix} U_\alpha \\ T_{p2} \\ T_{p3} \end{bmatrix}$$

Here the torque acting along the first axis is due to the damping effect of the PTO for the motion of the flap relative to the hull therefore $U_\alpha = -k_{pto}\dot{\alpha}$ where k_{pto} is a positive constant for the PTO.

$$\begin{aligned} \mathbf{e}_1^T T_p &= U_\alpha \\ \mathbf{e}_1^T T_p &= -k_{pto}\dot{\alpha} \end{aligned}$$

The Torque acting on the hull due to the reaction at the pivot point relative to the \mathbf{b}_0' frame is $-R_f T_p$. Similarly, the force acting on the flap at the pivot point be F_p relative to the \mathbf{b}' frame and the force acting on the hull relative to \mathbf{b}_0' frame is $-R_f F_p$ where,

$$F_p = \begin{bmatrix} F_{p1} \\ F_{p2} \\ F_{p3} \end{bmatrix}$$

The weight acting on the on the center of masses of the hull and flap in frames \mathbf{b}_0' and \mathbf{b}' can be taken as F_{g0} and F_g respectively where,

$$F_{g0} = -R_0^T (Mg\mathbf{e}_3), F_g = -R^T (mg\mathbf{e}_3)$$

Where $\mathbf{e}_3 = [0 \ 0 \ 1]^T$

Therefore if the total torque acting on the flap about the pivot point in \mathbf{b}' frame is T_f

$$T_f = -l_f \times F_g$$

And the total force acting on the flap relative to the inertial frame of reference, f_f is ,

$$f_f = mg\mathbf{e}_3 + RF_p$$

Similarly, the total torque acting on the hull about its center of mass relative to \mathbf{b}_0 , T_0 is,

$$T_0 = -l_h \times R_f F_p - R_f T_p + T_e$$

Where $T_e = R_0 \tau_e$ is the external torque acting on the hull due to its interaction with the waves relative to \mathbf{b}_0 and τ_e is the torque relative to the inertial frame of reference.

And the force acting on the hull relative to the inertial frame of reference, f_0 is,

$$f_0 = Mg\mathbf{e}_3 - RF_p + f_e$$

Where f_e is the external force acting on the hull.

Here $g = -9.81 \text{ ms}^{-2}$ is the acceleration due to gravity.

Equations of motion

For the hull, Since the position of the center of mass of the hull relative to the inertial frame of reference is O , For the motion of the center of mass of the hull,

$$\begin{aligned} f_0 &= M\ddot{O} \\ Mg\mathbf{e}_3 - RF_p + f_e &= M\ddot{O} \end{aligned} \tag{1}$$

For the rigid body motion of the hull relative to frame \mathbf{b}_0 ,

$$\begin{aligned}\mathbb{I}_0 \dot{\Omega}_0 &= \mathbb{I}_0 \Omega_0 \times \Omega_0 + T_0 \\ \mathbb{I}_0 \dot{\Omega}_0 &= \mathbb{I}_0 \Omega_0 \times \Omega_0 - l_h \times R_f F_p - R_f T_p + T_e\end{aligned}\quad (2)$$

If the position of the center of mass of the flap relative to the inertial frame of reference is x ,

$$x = O - R_0 l_h + R l_f$$

Therefore,

$$\begin{aligned}\dot{x} &= \dot{O} - R_0 \hat{\Omega}_0 l_h + R \hat{\Omega} l_f \\ \ddot{x} &= \ddot{O} - R_0 \hat{\Omega}_0^2 l_h - R_0 \dot{\hat{\Omega}}_0 l_h + R \hat{\Omega}^2 l_f + R \dot{\hat{\Omega}} l_f \\ \ddot{x} &= \ddot{O} - R_0 \left(\hat{\Omega}_0^2 + \dot{\hat{\Omega}}_0 \right) l_h + R \left(\hat{\Omega}^2 + \dot{\hat{\Omega}} \right) l_f\end{aligned}$$

Therefore, for the motion of the center of mass of the flap is given by

$$\begin{aligned}f_f &= m \ddot{x} \\ m g \mathbf{e}_3 + R F_p &= m \left[\ddot{O} - R_0 \left(\hat{\Omega}_0^2 + \dot{\hat{\Omega}}_0 \right) l_h + R \left(\hat{\Omega}^2 + \dot{\hat{\Omega}} \right) l_f \right]\end{aligned}\quad (3)$$

For the rigid body motion of the flap, relative to frame \mathbf{b} ,

$$\begin{aligned}\mathbb{I} \dot{\Omega} &= \mathbb{I} \Omega \times \Omega + T_f \\ \mathbb{I} \dot{\Omega} &= \mathbb{I} \Omega \times \Omega + T_p - l_f \times F_p\end{aligned}\quad (4)$$

Obtaining a set of differential equations

From 1, 2 removing F_p

$$\mathbb{I}_0 \dot{\Omega}_0 = \mathbb{I}_0 \Omega_0 \times \Omega_0 - R_f T_p + T_e - l_h \times R_0^T (M g \mathbf{e}_3 - M \ddot{O} + f_e) \quad (5)$$

From 3, 4 removing F_p

$$\begin{aligned}\mathbb{I} \dot{\Omega} &= \mathbb{I} \Omega \times \Omega + T_p - l_f \times m R^T \left[\ddot{O} - g \mathbf{e}_3 - R_0 \left(\hat{\Omega}_0^2 + \dot{\hat{\Omega}}_0 \right) l_h + R \left(\hat{\Omega}^2 + \dot{\hat{\Omega}} \right) l_f \right] \\ \mathbb{I} \dot{\Omega} &= \mathbb{I} \Omega \times \Omega + T_p + m l_f \times \left[R^T (g \mathbf{e}_3 - \ddot{O}) + R_f^T \left(\hat{\Omega}_0^2 + \dot{\hat{\Omega}}_0 \right) l_h \right] + m \left(-l_f \times \hat{\Omega}^2 l_f \right) + m \left(-l_f \times \dot{\hat{\Omega}} l_f \right)\end{aligned}$$

Considering properties of cross product,

$$X \times \dot{\hat{\Omega}} X = -X \times X \times \dot{\hat{\Omega}} = -\hat{X}^2 \dot{\hat{\Omega}}$$

also,

$$X \times \hat{\Omega}^2 X = X \times X \times \Omega \times \Omega = \hat{X}^2 \Omega \times \Omega$$

Defining $\tilde{\mathbb{I}} = \mathbb{I} - m \hat{l}_f^2$

$$\begin{aligned}\mathbb{I} \dot{\Omega} - m \hat{l}_f^2 \dot{\hat{\Omega}} &= \mathbb{I} \Omega \times \Omega + T_p + m l_f \times \left[R^T (g \mathbf{e}_3 - \ddot{O}) + R_f^T \left(\hat{\Omega}_0^2 + \dot{\hat{\Omega}}_0 \right) l_h \right] - m \hat{l}_f^2 \Omega \times \Omega \\ \tilde{\mathbb{I}} \dot{\Omega} &= \tilde{\mathbb{I}} \Omega \times \Omega + T_p + m l_f \times \left[R^T (g \mathbf{e}_3 - \ddot{O}) + R_f^T \left(\hat{\Omega}_0^2 + \dot{\hat{\Omega}}_0 \right) l_h \right]\end{aligned}\quad (6)$$

From 1 and 3

$$(M+m)g\mathbf{e}_3 + f_e = (M+m)\ddot{O} + m \left[-R_0 \left(\hat{\Omega}_0^2 + \dot{\hat{\Omega}}_0 \right) l_h + R \left(\hat{\Omega}^2 + \dot{\hat{\Omega}} \right) l_f \right] \quad (7)$$

Since there are 6 variables that needs to be solved by the ODEs, $(\ddot{\theta}, \ddot{\alpha}, \text{ and } \ddot{O})$, and since $\mathbf{e}_1^T T_p$ is known, 5 and 6 can be multiplied by \mathbf{e}_1^T to obtain 2 equations and 7 will give 3 equations this will give the 6 equations required to solve the variables. Also recall that, $\Omega_0 = \dot{\theta} \mathbf{e}_1$ and $\Omega = (\dot{\theta} + \dot{\alpha}) \mathbf{e}_1$ (hence $\hat{\Omega}_0 = \dot{\theta} \hat{\mathbf{e}}_1$ and $\hat{\Omega} = \dot{\theta} \hat{\mathbf{e}}_1$) Therefore the equations are,

From 7

$$(M+m)\ddot{O} - mR_0\dot{\hat{\Omega}}_0 l_h + mR\dot{\hat{\Omega}} l_f = (M+m)g\mathbf{e}_3 + mR_0\hat{\Omega}_0^2 l_h - mR\hat{\Omega}^2 l_f + f_e$$

$$(M+m)\ddot{O} + m(R\hat{\mathbf{e}}_1 l_f - R_0\hat{\mathbf{e}}_1 l_h) \ddot{\theta} + mR\hat{\mathbf{e}}_1 l_f \ddot{\alpha} = (M+m)g\mathbf{e}_3 + m(R_0\hat{\Omega}_0^2 l_h - R\hat{\Omega}^2 l_f) + f_e \quad (8)$$

From 5

$$\mathbf{e}_1^T R_f^T \left[\mathbb{I}_0 \dot{\Omega}_0 - M \hat{l}_h R_0^T \ddot{O} \right] = \mathbf{e}_1^T R_f^T \left[\mathbb{I}_0 \Omega_0 \times \Omega_0 - R_f T_p + T_e - l_h \times R_0^T (Mg\mathbf{e}_3 + f_e) \right]$$

$$-M\mathbf{e}_1^T R_f^T \hat{l}_h R_0^T \ddot{O} + (\mathbf{e}_1^T R_f^T \mathbb{I}_0 \mathbf{e}_1) \ddot{\theta} = \mathbf{e}_1^T R_f^T \left[\mathbb{I}_0 \Omega_0 \times \Omega_0 + T_e - l_h \times R_0^T (Mg\mathbf{e}_3 + f_e) \right] + k_{pto} \dot{\alpha} \quad (9)$$

From 6

$$\mathbf{e}_1^T \left[\tilde{\mathbb{I}} \dot{\Omega} + m \hat{l}_f R^T \ddot{O} + m \hat{l}_f R_f^T \dot{\hat{\Omega}}_0 l_h \right] = \mathbf{e}_1^T \left[\tilde{\mathbb{I}} \Omega \times \Omega + m l_f \times \left(R^T g\mathbf{e}_3 + R_f^T \hat{\Omega}_0 l_h \right) + T_p \right]$$

$$\mathbf{e}_1^T \tilde{\mathbb{I}} \mathbf{e}_1 (\ddot{\theta} + \ddot{\alpha}) + m \mathbf{e}_1^T \hat{l}_f R^T \ddot{O} + m \mathbf{e}_1^T \hat{l}_f R_f^T \hat{\mathbf{e}}_1 l_h \ddot{\theta} = \mathbf{e}_1^T \left[\tilde{\mathbb{I}} \Omega \times \Omega + m l_f \times \left(R^T g\mathbf{e}_3 + R_f^T \hat{\Omega}_0 l_h \right) \right] - k_{pto} \dot{\alpha}$$

$$m \mathbf{e}_1^T \hat{l}_f R^T \ddot{O} + \mathbf{e}_1^T \left(\tilde{\mathbb{I}} \mathbf{e}_1 + m \hat{l}_f R_f^T \hat{\mathbf{e}}_1 l_h \right) \ddot{\theta} + \mathbf{e}_1^T \tilde{\mathbb{I}} \mathbf{e}_1 \ddot{\alpha} = \mathbf{e}_1^T \left[\tilde{\mathbb{I}} \Omega \times \Omega + m l_f \times \left(R^T g\mathbf{e}_3 + R_f^T \hat{\Omega}_0 l_h \right) \right] - k_{pto} \dot{\alpha} \quad (10)$$

Then if we take,

$$\begin{bmatrix} v \\ \omega_0 \\ \omega \end{bmatrix} = \begin{bmatrix} \dot{O} \\ \dot{\theta} \\ \dot{\alpha} \end{bmatrix} \quad \text{and} \quad X = \begin{bmatrix} v \\ \omega_0 \\ \omega \\ \theta \\ \alpha \end{bmatrix}$$

Where v, ω_0, ω are velocity of the center of mass of the body, angular velocity of rotation of the hull and the angular velocity of rotation of the flap relative to the hull respectively.

Therefore if

$$A = \begin{bmatrix} (M+m)\mathbf{I}_{3 \times 3} & m(R\hat{\mathbf{e}}_1 l_f - R_0\hat{\mathbf{e}}_1 l_h) & mR\hat{\mathbf{e}}_1 l_f & \mathbf{0}_{3 \times 3} & \mathbf{0}_{3 \times 1} & \mathbf{0}_{3 \times 1} \\ -M\mathbf{e}_1^T R_f^T \hat{l}_h R_0^T & \mathbf{e}_1^T R_f^T \mathbb{I}_0 \mathbf{e}_1 & 0 & \mathbf{0}_{1 \times 3} & 0 & 0 \\ m\mathbf{e}_1^T \hat{l}_f R^T & \mathbf{e}_1^T (\tilde{\mathbb{I}} \mathbf{e}_1 + m \hat{l}_f R_f^T \hat{\mathbf{e}}_1 l_h) & \mathbf{e}_1^T \tilde{\mathbb{I}} \mathbf{e}_1 & \mathbf{0}_{1 \times 3} & 0 & 0 \\ \mathbf{0}_{3 \times 3} & \mathbf{0}_{3 \times 1} & \mathbf{0}_{3 \times 1} & \mathbf{I}_{3 \times 3} & \mathbf{0}_{3 \times 1} & \mathbf{0}_{3 \times 1} \\ \mathbf{0}_{1 \times 3} & 0 & 0 & \mathbf{0}_{1 \times 3} & 1 & 0 \\ \mathbf{0}_{1 \times 3} & 0 & 0 & \mathbf{0}_{1 \times 3} & 0 & 1 \end{bmatrix}$$

and,

$$F = \begin{bmatrix} (M+m)g\mathbf{e}_3 + m(R_0\hat{\mathbf{e}}_1^2 l_h \omega_0^2 - R\hat{\mathbf{e}}_1^2 l_f (\omega + \omega_0)^2) + f_e \\ \mathbf{e}_1^T R_f^T [\omega_0^2 \mathbb{I}_0 \mathbf{e}_1 \times \mathbf{e}_1 + T_e - l_h \times R_0^T (Mg\mathbf{e}_3 + f_e)] + k_{pto} \omega \\ \mathbf{e}_1^T [(\omega + \omega_0)^2 \tilde{\mathbb{I}} \mathbf{e}_1 \times \mathbf{e}_1 + m l_f \times (R^T g\mathbf{e}_3 + R_f^T \hat{\mathbf{e}}_1 l_h \omega_0)] - k_{pto} \omega \\ v \\ \omega_0 \\ \omega \end{bmatrix}$$

The set of ordinary differential equations that need to be solved to obtain X as the solution are,

$$\begin{aligned}\dot{X} &= A^{-1}F \\ R_f &= R_1(\alpha) \\ R_0 &= R_1(\theta) \\ R &= R_0 R_f\end{aligned}$$

Therefore if X can be calculated for a particular time period, the motion of the object can be determined under the external force f_e and external torque T_e which may vary with time. Here, these values are taken to be sinusoidal as it is placed on sea waves.

References

- [1] Josh Davidson and John V. Ringwood. Matheatical Modelling of Mooring Systems for Wave Energy Converters-A Review. *Energies*, 10.
- [2] Prasanna Gunawardane, Sudesh Ratnayake, and Tomiji Watabe. New Hybrid HST Pump Development for Wave Energy Applications-Study on the Slipper Bearing of an Axial Piston Pump.
- [3] Pozzi Nicola, Bracco Giovanni, Passione Biagio, Sirigu Sergej Antonello, , and Giuliana Mattiazzo. PeWEC: Experimental validation of wave to PTO numerical model. *Ocean Engineering*, 2018.
- [4] Pozzi Nicola, Bracco Giovanni, Passione Biagio, Sirigu Sergej Antonello, Vissio Giacomo, and Mattiazzo Giuliana. Wave Tank Testing of a Pendulum Wave Energy Converter 1:12 Scale Model. *International Journal of Applied Mechanics*, 9, March 2017.